Western&Graduate&PostdoctoralStudies

Electronic Thesis and Dissertation Repository

8-23-2019 10:00 AM

The role of kidney injury molecule-1 in the metastasis of renal cell carcinoma

Jasper Lee, *The University of Western Ontario*

Supervisor: Gunaratnam, Lakshman, *The University of Western Ontario*
A thesis submitted in partial fulfillment of the requirements for the Master of Science degree in Microbiology and Immunology
© Jasper Lee 2019

Follow this and additional works at: https://ir.lib.uwo.ca/etd

Part of the Disease Modeling Commons, and the Neoplasms Commons

Abstract

Over 30% of patients with renal cell carcinoma (RCC) present with metastases, with median survival of 2 years. Kidney injury molecule 1 (KIM-1) is a cell-surface glycoprotein expressed by >90% of RCC tumours. Preliminary data mined from The Cancer Genome Atlas RNA-sequencing database indicates that KIM-1 overexpression predicts overall survival in patients. Here we sought to determine if tumour KIM-1 plays a role in RCC cell extravasation and metastasis to the lungs. *In vitro* invasion and *in vivo* metastasis assays were performed to investigate the metastatic potential of KIM-1-expressing cells, and RNA-seq was conducted to identify differentially expressed genes between KIM-1$^+$ and KIM-1^{neg} cells.

Invasion was significantly decreased *in vitro* in both murine and human RCC cells that expressed KIM-1. We concluded that KIM-1 inhibits RCC extravasation and metastasis to the lungs, independent of adaptive immunity. RNA-seq analysis provided putative downstream effectors of KIM-1.

Lay Summary

Metastasis is often the deadliest aspect of cancer and is characterized by the secondary spread of cancer cells to distant sites of the body from the primary tumour. Over a third of patients with renal cell carcinoma (RCC) - the most common form of kidney cancer - present with metastases at the time of diagnosis. Kidney injury molecule 1 (KIM-1) is a cell-surface protein expressed by >90% of RCC tumours. Preliminary data from our lab indicates that KIM-1 overexpression predicts overall survival in patients. Here we sought to determine if tumour KIM-1 plays a role in RCC metastasis to the lungs - the most common site of metastasis in RCC. The metastatic potential of KIM-1-expressing cells was investigated, and the differences in gene expression between KIM-1$^+$ and KIM-1^{neg} cells were analyzed.

We concluded that KIM-1 inhibits RCC invasion and metastasis to the lungs, independent of the adaptive immune system. RNA-sequencing analysis of the genes provided putative downstream effectors of KIM-1, which could serve as novel therapeutic targets for the treatment of metastatic RCC.

Keywords

Kidney injury molecule-1 (KIM-1), renal cell carcinoma, cancer, invasion, extravasation, metastasis, lung metastasis, murine, Renca, 786-O

Co-Authorship Statement

This thesis was supervised and edited by Dr. Lakshman Gunaratnam, who contributed to the planning and design of experiments, as well as the supply of the necessary animals, equipment and reagents.

Acknowledgments

I would like to thank first and foremost, my supervisor Dr. Lakshman Gunaratnam for his guidance and patience throughout my thesis. Without him, I would not have had such a fascinating project or the opportunity to call this project my own. He has provided me with mentorship when I needed it most and given me the necessary encouragement to persevere when I felt lost and dejected. I am forever grateful for his patience and belief in me, and his genuine interest for my success and well-being. His kind words and reassuring attitude reignited my passions when I was at my lowest and made me feel proud of my work and progress. He has taught me the invaluable skill of *how* to think critically and outside of the box, rather than *what* to think. Thank you for giving me the freedom and independence to grow and learn on my own, and an environment to flourish in. His personal successes and philanthropy have inspired me to contemplate my own priorities which continue to drive me each and every day. I thoroughly enjoyed the social charity events he has invited me to, which revealed to me another side of the research/physician world. One of my favourite things about Dr. G that I will never forget were his big whole-hearted laughs which always brought a smile to my face. Thank you Dr. Gunaratnam for being the best supervisor a student could ask for and making my M.Sc. journey such a delightful one.

I would like to extend a special thank you to Marie Sarabusky (Western University) for her contributions to my project. Her work generating the stable Kim-1 Renca cells, and KIM-1 knock-down 786-O cells (Appendix A 3-5) was substantial to my project and paved the foundations for my thesis. Additionally, her work, along with Dr. Hon Leong (University of Toronto), and Fabrice Lucien (Mayo Clinic) with the CAM model has provided me with the fundamental extravasation data presented in this thesis (Figure 5). Furthermore, I would like to thank Marie for her invaluable advice during my transition into graduate school.

Next, I would like to thank Audrey Champagne (CHU de Québec-Université) for her work in mining TCGA Illumina RNA-seq database (Appendix A 1), which has provided me with preliminary data to base the rationale of my thesis on.

Words cannot describe the amount of gratitude I have for the members of my laboratory. Dr. Xizhong Zhang, you are the backbone of our group at the Matthew Mailing Centre. Without

you helping organize and manage equipment, mice, and reagents, I would not have gotten through my M.Sc. as smoothly as I did. Brad Shrum, thank you for your guidance and management at SDRI. I regret not being at SDRI more to engage in fun and philosophical life chats. Dr. Elena Tutunea-Fatan, thank you for being such a kind and patient mentor, and teaching me how to run Transwell assays. Thank you, Ji Yun Lee, for being my first friend in the lab and helping me with all my tail-vein injections. Without you, I would have a lot less data to show, and a lot less gossip to indulge in. You are such a kind and supportive friend, and I'm glad I could be the catalyst for you and Josh. Thank you Yutong Zou for your invaluable expertise with my orthotopic kidney injections and always being so friendly. Saranga Sriranganathan, thank you for being a beacon of light for me while I was writing this thesis, and thank you for always engaging in thought-provoking conversations with me. Your innocence and willingness to learn are inspiring traits I wish I shared. Thank you for being such a thoughtful friend and for always having good intentions. Demitra Yotis a.k.a tomato head, thank you for listening to all my rants and deep philosophical discussions during those long car rides, and for bringing so much life to our lab. Thank you for being such an easy target to make fun of for a good laugh and for providing me with an unexpected but much-welcomed friendship. Ingrid Hon, thank you for being such an easy-going lab mate and making MMC a comfortable workspace.

I would like to thank the members of my advisory committee: Dr. Nicholas Power, Dr. Mansour Haeryfar, and Dr. Zhuxu Zhang, for their generous time and contributions to my project. Your guidance and insight on different aspects of my project helped shape my thesis into what it is today. Nick, thank you for your kind words from the beginning. You believed in my project, and in my abilities to make a fascinating new story out of it. I am forever grateful for the input you have given me. Dr. Haeryfar, thank you for your expertise on the immune components of my project, and for asking the right questions to not only stimulate me to think, but to push my project towards the right direction. Dr. Zhang, thank you for your kind and gentle demeanor throughout my project, and for your invaluable input on how to better run my experiments.

A big thank you goes out to the entire Microbiology and Immunology department; students and faculty, for giving me so many new friendships and memorable experiences. Thank you, Dr. Kelly Summers and Dr. Sung Kim, for giving me the opportunity to be a graduate

Table of Contents

Abbreviations

ADP	Adenosine Diphosphate
AIM	Apoptosis Inhibitor of Macrophages
AKI	Acute Kidney Injury
AP-1	Activating Protein 1
ARF6	ADP-Ribosylation Factor 6
BCA	Bicinchoninic Acid
BLI	Bioluminescence Imaging
CAM	Chorio-Allantoic Membrane
ccRCC	Clear Cell Renal Cell Carcinoma
cDNA	Complementary Deoxyribose Nucleic Acid
CKD	Chronic Kidney Disease
CTLA-4	Cytotoxic T Lymphocyte Antigen 4
CXCR4	C-X-C Motif Chemokine Receptor 4
CXCL12/SDF1	C-X-C Motif Chemokine Ligand 12/Stromal cell-derived factor 1
DMEM	Dulbecco's Modified Eagle Medium
ECM	Extracellular Matrix
EFA6	Exchange Factor for ARF6
EMT	Epithelial-Mesenchymal-Transition
FBS	Fetal Bovine Serum
G418	Geneticin Sulfate
$Ga_{12/13}$	Alpha subunit of heterotrimeric G protein 12/13
GAP	GTPase Activating Protein
GPCR	G Protein-Coupled Receptor
GTP	Guanosine Triphosphate
GTPase	Guanosine Triphosphatase
HAVCR1	Hepatitis A Virus Cellular Receptor 1
HIF	Hypoxia Inducible Factor
HRP	Horse Radish Peroxidase
IFN-γ	Interferon Gamma
IL-2	Interleukin 2
IL-6	Interleukin 6
Kim-1	Kidney Injury Molecule-1 (mouse)
KIM-1	Kidney Injury Molecule-1 (human) or *both* human and mouse when discussed together
LB	Lysogeny Broth
MMP	Matrix Metallopeptidase
MOI	Multiplicities of Infection
mTOR	Mammalian Target of Rapamycin
MYC/c-Myc	Cellular Myelocytomatosis Homology Oncogene
NK	Natural Killer

NKT	Natural Killer T Lymphocyte
NOD	Non-Obese Diabetic
ORF	Open Reading Frame
p53	Tumour Protein 53
PBS	Phosphate Buffered Saline
PD-1/L1	Programmed Death 1/Ligand 1
PS	Penicillin/Streptomycin
PTEC	Proximal Tubular Epithelial Cell
Rag1	Recombinase Activation Gene 1
Rap1	Ras-Associated Protein 1
RCC	Renal Cell Carcinoma
Renca	Renal Cell Adenocarcinoma
RPMI	Roswell Park Memorial Institute
RT	Room Temperature
rTKI	Receptor Tyrosine Kinase Inhibitors
RT-PCR	Real Time-Polymerase Chain Reaction
SCID	Severe Combined Immunodeficient
SDS	Sodium Dodecyl Sulfate
SEM	Standard Error of Mean
SFM	Serum Free Media
shRNA	Short Hairpin RNA
STAT3	Signal Transducer and Activator of Transcription 3
TCGA	The Cancer Genome Atlas
TEM	Trans-Endothelial Migration
TGF-β1	Transforming Growth Factor β1
TIM-1	T Cell Immunoglobulin and Mucin Domain 1
TME	Tumour Micro-Environment
TNM	Tumour Node Metastasis
TU	Transducing Units
VEGF	Vascular Endothelial Growth Factor
VHL	von Hippel-Lindau
WT	Wild-type
10%	Complete Media

List of Tables

List of Figures

Chapter 1

1 Introduction

1.1 Cancer

Cancer affects over 18 million people worldwide and is the second leading cause of death globally. An increase in its incidence is also evident, and can be attributed to various risk factors such as environment, poor diet, and inadequate physical activity (Ferlay, Soerjomataram et al. 2015). In 2012 alone, GLOBOCAN estimated 14.1 million new cases of cancer, and 8.2 million deaths due to cancer. In Canada, an estimated 2 in 5 Canadians will develop cancer in their lifetime, and 1 in 4 will die from their disease (Canadian Cancer Society 2015). Cancer is characterized as an uncontrolled proliferation and spread of abnormal cells, which may lead to death (American Cancer Society 2016). Metastasis is characterized by the spread of cancer cells from the primary tumour to distant tissues and organs, and the establishment of a tumour at the secondary site (Fidler 2003). Metastases are the most severe aspect of cancer, as they are the cause of the majority of deaths in cancer patients. One of the most prominent barriers to the treatment of metastatic cancer is the heterogeneity of cancer cells within the metastatic focus compared to the primary tumour (Fidler 2003).

Hanahan and Weinberg have proposed that there are six characteristics that are essential for the development and progression of all cancers, which they have termed the hallmarks of cancer (Figure 1) (Hanahan and Weinberg 2011). Together, these six hallmarks allow for the growth and dissemination of tumours: sustaining proliferative signaling, evading growth suppressors, inducing angiogenesis, resisting cell death, enabling replicative immortality, and activating invasion and metastasis. In recent years, they have suggested the addition of two emerging hallmarks: reprogramming of energy metabolism, and immune evasion. In addition to the hallmark characteristics, Hanahan and Weinberg have posited that enabling characteristics such as genomic instability and tumour-promoting inflammation are underlying factors that lead to the development of hallmark characteristics.

Research into the enigmatic steps of the invasion-metastasis cascade in recent years have yielded a greater understanding on this critical step of cancer progression. Technological advances have provided newer tools and models to investigate regulatory genes and pathways involved in invasion and metastasis and shed light on what was previously poorly understood.
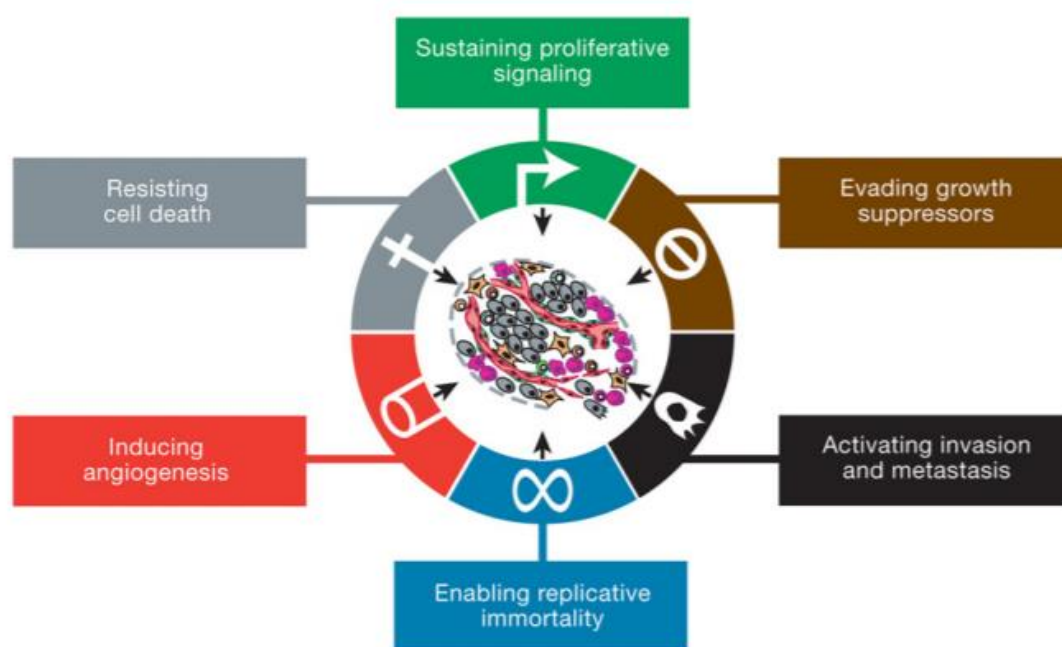
Figure 1. The hallmarks of cancer

The six hallmarks of cancer first posited by Hanahan and Weinberg in 2000. These hallmarks are necessary and essential capabilities that enable tumour growth and metastatic dissemination. Adapted with permission from (Hanahan and Weinberg 2011).

1.1.1   Invasion and Metastasis

Metastasis is a complex process, requiring the multi-step succession of events from the development of the primary tumour, detachment and degradation of the ECM, intravasation into the circulation, adhesion to the blood vessel wall, and finally extravasation into the secondary tissue (Figure 2). Invasion and extravasation are the crucial and penultimate steps in the spread of cancers.
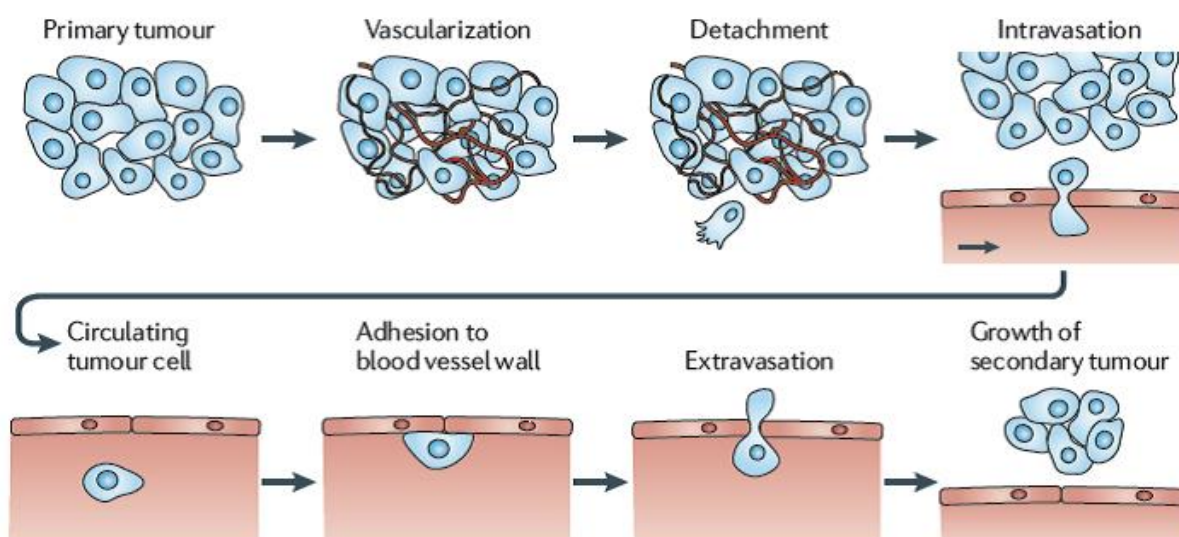
Figure 2. Steps in the process of metastasis

Metastasis is a complex process that requires multiple steps to occur in succession. Cells that successfully detach and enter the vasculature must survive various physical stressors before arresting on the endothelium at distal sites. The ability for cancer cells to extravasate is essential for the dissemination of cancer cells. Adapted with permission from (Wirtz, Konstantopoulos et al. 2011).

1.1.2   Epithelial-mesenchymal-transition and Anoikis

One critically important process during the dissemination of carcinomas is the process of epithelial-mesenchymal-transition (EMT) (Cao, Livas et al. 2016). EMT confers migratory and invasive properties upon cancer cells, as well as the ability to degrade the extracellular

matrix (ECM), allowing them to leave the primary tumour site and enter the vasculature (Lambert, Pattabiraman et al. 2017). Once cancer cells enter the circulation, they must overcome enormous physiological stressors before they can establish a metastatic focus at a distant site. Disseminated cancer cells must be able to resist physical stressors such as anoikis – a form of apoptosis due to detachment from the extracellular matrix – as well as shear stress (Lambert, Pattabiraman et al. 2017). Anoikis is a tumour suppressing mechanism that induces apoptosis in normal epithelial and endothelial cells that lose contact with the ECM and suppresses proliferation of transformed cells at ectopic sites (Rennebeck, Martelli et al. 2005). Resistance to anoikis is therefore essential to the survival and migration of malignant cells in the vasculature. Anoikis resistance in cancer cells is coupled with mechanisms that promote invasiveness which allow disseminated cells to migrate to distal sites and establish metastases (Zhu, Sanchez-Sweatman et al. 2001, Sakamoto, McCann et al. 2010). Along with the physical impediments, cancer cells will encounter a plethora of cell types; among them, platelets, neutrophils, and NK cells, which may serve to facilitate their passage or swiftly end their journey (Lambert, Pattabiraman et al. 2017).

1.1.3   Arrest and Extravasation

One of the final obstacles malignant cells must overcome is the process of trans-endothelial migration (TEM). Cancer cells must gain the ability to extravasate out of the bloodstream and into the secondary tissue sites. Often, this occurs in small capillaries where the cancer cells are physically confined to narrow luminal spaces, where they form stable interactions with adhesion molecules on endothelial cells (Reymond, d'Agua et al. 2013). Studies have shown that cancer cells may roll along the endothelium until stable adhesions form between tumour cells and endothelial cells, by action of selectins, cadherins, and integrins (Miles, Pruitt et al. 2008, Stoletov, Kato et al. 2010). Integrins are a group of cell-surface proteins that enable cells to attach to the extracellular matrix (ECM), and sense whether adhesion has occurred; β1-integrins specifically, have been shown to be crucial for mediating the dynamic remodeling of endothelial cell junctions (Stoletov, Kato et al. 2010), through the actions of Rho-GTPases (Miles, Pruitt et al. 2008).

1.1.4   Rho-GTPases in Cancer

Rho-GTPases regulate cytoskeletal changes necessary for TEM by modulating actin filament assembly (Braga, Del Maschio et al. 1999, Miles, Pruitt et al. 2008). Calcium-dependent cadherin molecules are a family of molecules that contribute to cell-cell adhesion. Cadherins line the extracellular domains of epithelial and endothelial cells and hold cells together through homophilic interactions (Lozano, Betson et al. 2003). Actin reorganization by Rho-GTPases alters the stability of endothelial cell-cell junctions – known as adherens junctions – by interacting with the cytoplasmic ends of cadherin molecules and disrupting the cell-cell interactions (Miles, Pruitt et al. 2008). Additionally, Rho-GTPases may also regulate cancer cell motility through the same process of actin reorganization. The disruption of cadherin-mediated adhesion is known to be one of the most efficient mechanisms to achieve EMT, and Rho-GTPases have been shown to be necessary for the maintenance of said cadherin-mediated adhesions (Braga 2000, Lozano, Betson et al. 2003). Disruptions in both cadherin expression and function, as well as deregulations in Rho-GTPases are thought to be required for TEM to occur.

1.1.5   Chemokines in Cancer

Chemokines also play a major role in invasion and metastasis, through their interactions with G protein-coupled receptors (GPCR). It is well understood that certain cancer types metastasize to specific secondary sites; prostate cancers preferentially metastasize to the bone; lung cancers preferentially metastasize to the bone, liver and brain; breast cancers preferentially metastasize to the lung, bone, liver, and brain; pancreatic cancers preferentially metastasize to the liver; and kidney cancers preferentially metastasize to the lungs, bone, and lymph nodes (Patanaphan, Salazar et al. 1988, Edlund, Sung et al. 2004, Hess, Varadhachary et al. 2006, Bianchi, Sun et al. 2012). The seed-and-soil hypothesis helps to partly explain these metastatic patterns through the understanding of the expression of chemokines and their receptors between target sites and cancer cells. Of all the chemokines known, the CXCR4/CXCL12 axis is most often implicated in tumour progression, metastasis, and survival (Teicher and Fricker 2010). CXCR4 is an alpha-chemokine receptor that is normally absent or expressed at low levels, and only overexpressed by malignant epithelial cells (Balkwill 2004). It is believed that the

expression of CXCL12, also known as stromal-derived-factor-1 (SDF-1), by the target endothelium attracts cancer cells expressing its cognate receptor CXCR4 and stimulates their extravasation into secondary tissues. Studies have demonstrated the homing effect that CXCL12 has on CXCR4^{+} cancer cells, showing that the CXCR4/CXCL12 axis has no effect on adhesion, but significantly enhances tumour cell extravasation (which was accompanied by the activation of Rho-GTPases) (Gassmann, Haier et al. 2009, Teicher and Fricker 2010). The continued expression of these chemokines acts as a component of the "soil" to retain the "seeds" that have made the pilgrimage from their primary tumours, and promote angiogenesis, proliferation, and survival (Balkwill 2004, Teicher and Fricker 2010).

1.2 Renal Cell Carcinoma

Kidney cancer is the eighth most common form of cancer, and the twelfth leading cause of deaths due to cancer (De, Otterstatter et al. 2014). Renal cell carcinoma (RCC) is the most common form and accounts for over 90% of all cases of kidney cancer, with a 5-year survival rate of 72% at the time of diagnosis (De, Otterstatter et al. 2014). Depending on tumour progression, survival rates can be considerably lower in patients with metastatic forms of the disease. These survival rates are drastically reduced in patients diagnosed with stage IV of the disease – characterized by the metastasis of the tumour to distant sites – to a mere 8% (American Cancer Society 2016). Due to a lack of effective screening tests for the early stages of the disease, over 30% of patients present with metastases at the time of diagnosis (Canadian Cancer Society 2015).

1.2.1 Risk Factors and Causes of RCC

Risk factors for RCC development include smoking, obesity, having first-degree relatives with the disease, as well as a genetic mutation of the von Hippel-Lindau (VHL) protein (De, Otterstatter et al. 2014). Of the RCC subtypes, the clear cell variant (ccRCC) accounts for more than 80% of them (De, Otterstatter et al. 2014). The majority of ccRCCs have a loss-of-function mutation in a gene on chromosome 3, which codes for the VHL protein, a tumour suppressor known to mediate proteasomal degradation; one of its best known targets is the alpha subunit of hypoxia inducible factors (HIF) (Kumar and Gabrilovich

2014). An accumulation of HIFs is associated with increased expression of vascular endothelial growth factor (VEGF) and other angiogenic factors – conditions typically seen in pre-malignant lesions (Kumar and Gabrilovich 2014, Schodel, Grampp et al. 2016). Two isoforms of hypoxia-inducible factor alpha exist: HIF-1α and HIF-2α. Unique to ccRCC, it has been shown that the two HIFα isoforms have opposing effects, with HIF-1α acting as a tumour suppressor, and HIF-2α acting as an oncogene (Schodel, Grampp et al. 2016). It has been suggested that there is a HIF switch during the development of RCC, where HIF-1α drives the acute response to hypoxia, and HIF-2α drives the chronic response to hypoxia (Koh and Powis 2012). Both HIF isoforms are activated under pseudohypoxic conditions due to the loss of VHL, but there is a gradual loss of HIF-1α expression, coupled with an increase in HIF-2α expression as tumour grade increases (Raval, Lau et al. 2005, Koh and Powis 2012). The oncogenic HIF-2α has been implicated in the deregulation of numerous target genes which affect proliferation including MYC, TGF-α, VEGF, and p53 (Gunaratnam, Morley et al. 2003, Schodel, Grampp et al. 2016). Studies have demonstrated the contrasting effects between the HIF isoforms, indicating that HIF-2α enhances tumour growth, whereas HIF-1α inhibits c-Myc activity and RCC proliferation (Raval, Lau et al. 2005, Gordan, Lal et al. 2008). Given the fact that loss of HIF-1α was a notable hallmark of renal cell carcinoma, downregulation of HIF-1α is believed to be important in the pathogenesis of ccRCC. Indeed, Shen et al. (2011) found that the downregulation of HIF-1α is associated with enhanced tumour growth in ccRCC, implicating it as a tumour suppressor (Shen, Beroukhim et al. 2011).

Additionally, it has been shown that mutations in the VHL gene leads to upregulation of CXCR4 expression in RCC (Staller, Sulitkova et al. 2003). VHL normally acts as a tumour suppressor and negatively regulates CXCR4 expression via the degradation of HIF. However, when mutated, or under hypoxic conditions, HIF can induce CXCR4 expression. Overexpression of CXCR4 in RCC tumours is also associated with poor prognoses (Staller, Sulitkova et al. 2003, Zagzag, Krishnamachary et al. 2005). Another study demonstrated that the increased chemotactic response of CXCR4^{+} cancer cells towards CXCL12 expressing targets is dependent on the stabilization of CXCR4 transcripts and the activation of HIF (Schioppa, Uranchimeg et al. 2003). Zagzag et. Al. found that the loss-of-function

of VHL was responsible for the upregulation of both CXCR4 and its ligand CXCL12 (Zagzag, Krishnamachary et al. 2005).

G proteins and GPCRs such as $G\alpha_{12}$ and $G\alpha_{13}$ are known to promote proliferation and metastasis in a variety of cancers (Dorsam and Gutkind 2007). In RCC, GTP-bound (active) $G\alpha_{12}$ has been shown to bind to exchange factor for ARF6 (EFA6) and activate the ADP-ribosylation factor 6 (ARF6)-EFA6 pathway, which subsequently results in the process of EMT and the promotion of invasion and metastasis (Hashimoto, Mikami et al. 2016). $G\alpha_{12/13}$ have also been shown to regulate TGF-β1 (a known inducer of EMT) expression through a Rho/Rac-dependent pathway via activating protein-1 (AP-1) (Lee, Yang et al. 2009). It has been suggested that the upregulation of TGF-β1 results in increased matrix metallopeptidase (MMP) expression – proteases which play major roles in metastasis by degrading the ECM (Zhu, Liang et al. 2017). In support of this, a study found that increased expression of MMPs in tumours is dependent on the activation of Rho and Rac (Lozano, Betson et al. 2003). A study in breast cancer demonstrated that CXCR4-mediated-chemotaxis and TEM of cancer cells is dependent on the coupling of $G\alpha_{13}$ to CXCR4, which activates the downstream cascade of Rho and promotes chemotaxis towards CXCL12-expressing organs and subsequent extravasation (Yagi, Tan et al. 2011). Although the study was done in breast cancer, the CXCR4/CXCL12 axis has also been documented to play a pathological role in promoting invasion and metastasis in RCC (Staller, Sulitkova et al. 2003, Zagzag, Krishnamachary et al. 2005). Lastly, $G\alpha_{13}$ has been shown to be responsible for proliferation, invasion, and EMT in RCC cells (Liu, Li et al. 2017). Inhibition of $G\alpha_{13}$ by the micro-RNA MiR-30b-5p effectively suppressed metastatic processes in RCC cell lines. Ultimately, there are many factors and molecules that contribute to the metastasis of RCC cells, and a greater knowledge of these molecular pathways would be beneficial in developing therapies to treating metastatic RCC.

1.2.2   Current Therapies for RCC

One of the major barriers to treating RCC currently is the ineffective detection of neoplasms at early stages of the disease, as one third of patients present with metastasis at diagnosis (Custodio, Joaquim et al. 2012). In localized forms of the disease, where the neoplasms are relatively small and metastases are not present, surgery is the most effective

form of therapy (de Vivar Chevez, Finke et al. 2014). Radical or partial nephrectomy in these patients significantly improves their 5-year survival rate. In patients with metastatic forms however, surgery *alone* yields no improvement on survival, only palliation and symptom relief (de Vivar Chevez, Finke et al. 2014). In metastatic cases, the most effective form of treatment is surgery in *conjunction* with molecular-targeted therapy and immunotherapy (de Vivar Chevez, Finke et al. 2014).

1.2.2.1   Molecular Targeted Therapy

Molecular targeted therapies act on molecules in the RCC pathway which are specific to the disease, hence minimizing toxicities and adverse effects on other organs and tissues (de Vivar Chevez, Finke et al. 2014). Silencing of the VHL gene in RCC results in the overexpression of VEGF which contributes to the angiogenic nature of the disease (de Vivar Chevez, Finke et al. 2014). VEGF and molecules along the VEGF pathway have been the focus of molecular targeted therapy and the mainstay treatment for metastatic RCC (Su, Stamatakis et al. 2014). Sunitinib is part of a class of drugs known as receptor tyrosine kinase inhibitors (rTKI), which exert their effects through the inhibition of VEGF receptors (Su, Stamatakis et al. 2014). Sunitinib has become a first-line treatment in advanced RCC patients due to its relatively high response rate of 40% and an extended survival of 40 months (Finke, Rayman et al. 2013). Studies have also found that sunitinib can deplete peripheral myeloid-derived suppressor cells (MDSC) and improve T cell functions in hosts (Finke, Rayman et al. 2013, Su, Stamatakis et al. 2014). Resistance to rTKIs arises in patients over time and is currently an area of focus.

The serine-threonine protein kinase mammalian target of rapamycin (mTOR) is a critical molecule in a multitude of biological pathways such as proliferation, metabolism, protein synthesis, and angiogenesis (de Vivar Chevez, Finke et al. 2014). Its expression is associated with worse outcomes in local and metastatic RCC patients (de Vivar Chevez, Finke et al. 2014). Two well-tested mTOR inhibitors: temsirolimus, and everolimus, are used as second-line treatment options in cases of disease progression after treatment with rTKIs and have demonstrated improvement in overall survival (Su, Stamatakis et al. 2014).

1.2.2.2 Immunotherapy

Immunotherapy is a form of cancer treatment which harnesses the host's own immune system to help eradicate the cancer. RCC is particularly amenable to immunotherapy owing to its immunogenic nature. While RCC elicits a strong immune response, RCC tumours evade immune destruction through a variety of mechanisms that ultimately render the activated immune cells entering the tumour dysfunctional (Massari, Santoni et al. 2015). Over a decade ago, high-dose interleukin-2 (IL-2) and interferon-gamma (IFN-γ) were the cytokine treatments of choice for metastatic renal cancer (Massari, Santoni et al. 2015). IL-2 promotes T cell proliferation and differentiation, whereas IFN-γ exerts anti-angiogenic effects, and promotes dendritic cell maturation (Raman and Vaena 2015). Although high-dose IL-2 therapy appeared promising, only a small population of patients showed stable curative responses. Due to the significant treatment-related toxicities associated with high-dose IL-2 therapy, only carefully selected patients were suitable for treatment (Raman and Vaena 2015). Clinical research has shifted towards alternative forms of immunotherapy with less adverse effects such as immune checkpoint inhibitors.

Ground breaking research and identification of the checkpoint inhibitors cytotoxic T lymphocyte antigen-4 (CTLA-4) and programmed death-1 (PD-1) have invited new possibilities for immunotherapy (Dong, Strome et al. 2002, Massari, Santoni et al. 2015). It is thought that CTLA-4 exerts its inhibitory effects during the priming and activation phase of T cells, whereas PD-1 exerts its inhibitory effects on effector T cells in the tumour microenvironment (TME) (Fife and Bluestone 2008, Massari, Santoni et al. 2015). PD-1 has two ligands: PD-L1 and PD-L2. PD-L1 is expressed on many cells throughout the body, whereas PD-L2 is only expressed on macrophages and dendritic cells (Massari, Santoni et al. 2015). PD-1 is expressed on many immune cells such as T cells, B cells, and NKT cells to prevent auto-immunity in inflammatory sites; a mechanism which tumours exploit by expressing PD-L1 on their surface to inhibit T cell responses and avoid immune destruction (Massari, Santoni et al. 2015). Research has also shown that PD-L1 is aberrantly expressed on primary and metastatic RCC tissue, and that its expression is associated with worse patient outcomes (Thompson, Dong et al. 2007). Research into PD-1/PD-L1 blockade therapy has shown promising results, with a well-studied anti-PD-1

antibody drug, nivolumab, producing a significant response rate of 27% in patients with RCC (Massari, Santoni et al. 2015). Nivolumab restores anti-tumour activity in patients and has been demonstrated to exert its activity within the TME (Philips and Atkins 2014). It has also been shown to produce relatively low levels of toxicity, accompanied with durable responses.

1.2.3   Murine Model for Renal Cell Carcinoma

The murine model for renal cell carcinoma is the most widely used model for studying the disease as it is the most analogous to the human form of the disease, thus treatments and responses can be effectively evaluated (Murphy and Hrushesky 1973). Two models are commonly used to study tumours in mice: the xenograft model and the syngraft model, which require immunodeficient and immunocompetent mice, respectively (White and Olsson 1980). The xenograft model requires either human RCC cell lines or a tumour graft from human samples, whereas in a syngraft model, the Renca cell line – derived from a spontaneously arising RCC cell line in BALB/c mice – is commonly used (Murphy and Hrushesky 1973). A disadvantage of cell lines is that they produce homogenous tumours, whereas human tumours are often heterogenous. An autochthonous murine model for ccRCC that recapitulates human ccRCC had long eluded scientists but recent groundbreaking work by Harlander et al. identified that mice harbouring combined *Vhl*, *Trp53* and *Rb1* mutations caused spontaneous ccRCC (Harlander, Schonenberger et al. 2017)**.** The study found that the mice developed genetically distinct ccRCC tumours and were molecularly similar to the human disease, thus providing a useful tool to investigate pre-clinical therapeutic studies.

1.2.3.1   Xenograft Model

In the xenograft model, fresh human tumours or established human cell lines can be successfully xenografted into immunodeficient mice and can propagate into solid tumours (White and Olsson 1980). The three most commonly used immunodeficient mouse strains are: nude athymic mice, which lack T cells; severe combined immunodeficient (SCID) mice, which lack B and T cells; and non-obese diabetic (NOD)/SCID mice, which lacks both B and T cells, and has decreased functional macrophages, granulocytes, and NK cells

(White and Olsson 1980). Human RCC cell lines are widely used in murine models to accurately study and characterize tumour development and progression, and has been important to understanding the cell biology of renal cancer (Morton and Houghton 2007). Currently, multiple human RCC cell lines are available: ACHN, A-498, 786-O, 769-P, Caki-1, and Caki-2 (Morton and Houghton 2007, Brodaczewska, Szczylik et al. 2016). Of the aforementioned cell lines, only A-498, 786-O, and 769-P have a VHL mutation, making them ideal choices to study ccRCC specifically. 786-O was one of the earliest established RCC cell lines and is most commonly used, as it also expresses elevated VEGF levels (Shinojima, Oya et al. 2007), a characteristic of ccRCC. The 769-P cell line also expresses high levels of VEGF, however, its use in xenograft models has been constrained as studies found it lacked tumourigenicity when injected subcutaneously or intravenously into mouse models (Kozlowski, Fidler et al. 1984, Miyake, Goodison et al. 2013). A major limitation of the xenograft model is the fact that the mice are immunodeficient, thus making it impossible to study the immune component of RCC and its interactions with the established tumours.

1.2.3.2   Syngraft Model

The syngraft model involves the establishment of immunologically compatible tumours in immunocompetent mice and is advantageous as it makes studying the interaction between immune cells and the tumours, as well as tumour progression and metastasis possible. The use of the Renca cell line in the RCC mouse model has been studied extensively since the 70s (Murphy and Hrushesky 1973). The growth and progression of the solid tumours follow a predictable timeline, as does the spread of secondary tumours. The growth and dissemination of the RCC tumours in this model are also consistent and reproducible, and strongly recapitulate the disease in humans, making the Renca cell line a popular model to use (Murphy and Hrushesky 1973). Furthermore, the Renca cell line reflects the immunogenic nature of human RCC, as repeated tumour challenges in mice resulted in decreased incidence.

1.2.4   Murine Model for Metastasis

To study metastasis in mice, three tumour transplant models are commonly used: the experimental metastasis model, the spontaneous metastasis model, and the genetically engineered mouse model (Gomez-Cuadrado, Tracey et al. 2017). For the purposes of this thesis, only the former two models will be discussed.

1.2.4.1   Experimental Metastasis Model

Experimental metastasis models allow for the rapid and reproducible development of metastases in specific organs (Gomez-Cuadrado, Tracey et al. 2017). Depending on the site of study, cancer cells can be injected intravascularly, and the route of injection determines the site of colonization (Khanna and Hunter 2005). For example; intravenous injections in the lateral tail vein result in lung metastases; intracardiac injections result in brain and bone metastases; and intraperitoneal injections result in ovarian metastases (Gomez-Cuadrado, Tracey et al. 2017). A major limitation of the experimental model is that they only reflect the late stages of the metastatic process, particularly the arrest and extravasation steps, and subsequent development of tumours in ectopic sites.

1.2.4.2   Spontaneous Metastasis Model

Spontaneous metastasis models on the other hand, allow for the metastatic disease to be studied in a manner that mimics the disease progression in humans. The cancer cells are transplanted orthotopically, and the entire metastatic cascade can be monitored as the primary tumour grows and disseminates naturally to the secondary site (Gomez-Cuadrado, Tracey et al. 2017). Orthotopic models can therefore recapitulate the disease in humans better as it allows cancers to interact with the tissue of origin and elicit natural responses, which also include the earlier stages of metastasis such as invasion and intravasation (Francia, Cruz-Munoz et al. 2011). Spontaneous models however, require greater expertise to implant the cancer cells properly in the orthotopic site (Gomez-Cuadrado, Tracey et al. 2017).

1.3   Kidney Injury Molecule

Kidney injury molecule-1 (KIM-1), also known as T cell immunoglobulin mucin domain 1 (TIM-1) and hepatitis A virus cellular receptor 1 (HAVCR1), belongs to the family of TIM proteins, which are type-1 cell surface glycoproteins involved in the regulation of T cell activation and tolerance (Han, Alinani et al. 2005), and is a highly upregulated marker in the proximal tubule after renal injury (Brodaczewska, Szczylik et al. 2016). It has a heavily glycosylated ectodomain that is cleaved and released into the lumen, and can be detected in the urine and blood of humans, mice, and rats following kidney injury (Ichimura, Bonventre et al. 1998, Sabbisetti, Waikar et al. 2014).

1.3.1   Function

Phosphatidylserine is expressed on the surface of apoptotic and necrotic cells (Fadok, Savill et al. 1992, Zargarian, Shlomovitz et al. 2017). KIM-1 is a phosphatidylserine receptor that transforms proximal tubular epithelial cells (PTEC) into semi-professional phagocytic cells that can recognize and enhance the clearance of apoptotic cells and necrotic cells, thus making it an important molecule in the regulation of the immune response after kidney injury (Ichimura, Asseldonk et al. 2008, Arai, Kitada et al. 2016). The rapid clearance of dead cells prevents excessive inflammation and auto-immune responses against intracellular antigens released from dying cells (Kobayashi, Karisola et al. 2007). Normally, KIM-1 preferentially binds and internalizes apoptotic cells over necrotic cells, but in the presence of the protein apoptosis inhibitor of macrophages (AIM), KIM-1-mediated clearance of necrotic cells is significantly increased (Molitoris 2014, Arai, Kitada et al. 2016). It has been shown that following kidney injury, AIM expression increases in the tubular lumen, where it binds necrotic debris and mediates phagocytosis by PTECs expressing KIM-1 (Arai, Kitada et al. 2016).

It has been suggested that KIM-1 can elicit opposite effects in the kidney; KIM-1 is protective early in acute kidney injury (AKI) (Yang, Brooks et al. 2015), but sustained expression leads to kidney fibrosis, progressive interstitial kidney inflammation, and chronic kidney disease (CKD), thus providing a potential link between AKI and CKD (Humphreys, Xu et al. 2013).

1.3.2   Role of KIM-1 in RCC

Following acute kidney injury, PTECs (including those expressing KIM-1) undergo de-differentiation, proliferation, and re-differentiation in order to repair the tubular epithelium (Humphreys, Xu et al. 2013). However, the de-differentiation of PTECs is heterogenous in nature, and only some of the regenerating cells express KIM-1 (Kusaba, Lalli et al. 2014). Similar to injured PTECs, RCC cells also exist in a state of de-differentiation (Shimazui, Oosterwijk-Wakka et al. 2000). Not surprisingly, KIM-1 is expressed in >90% of human RCC tissue samples (Bonventre 2014, Zhang, Mashni et al. 2014).

KIM-1 is highly expressed in the two most prevalent forms of RCC: clear cell RCC, and papillary RCC, and can serve as a non-invasive biomarker for the early diagnosis of the disease through the detection of the shed ectodomain in the urine of patients (Han, Alinani et al. 2005, Zhang, Mashni et al. 2014). Studies have shown that significantly greater levels of KIM-1 were detected in the urine samples of ccRCC patients compared with patients with prostate carcinoma or control subjects (Bonventre 2014, Zhang, Mashni et al. 2014). In contrast, KIM-1 is absent in normal kidney tissue, and it has been demonstrated that patients who tested positive for KIM-1 expression pre-nephrectomy showed either complete disappearance or marked reduction in KIM-1 expression post-nephrectomy (Han, Alinani et al. 2005, Bonventre 2014). It has recently been shown that plasma KIM-1 concentrations can serve as a reliable biomarker for the prediction of RCC onset up to 5 years before diagnosis (Scelo, Muller et al. 2018). Combined, these studies indicate that KIM-1 is a sensitive and specific biomarker for the early detection of RCC.

One study has shown that overexpression of KIM-1 promotes tumour growth in human 769-P cells, whereas silencing of the gene led to a reduction in cancer cell proliferation (Cuadros, Trilla et al. 2014). The same study found that KIM-1 activates the STAT-3/IL-6/HIF-1α axis in ccRCC, which indicates KIM-1s involvement in the pathway for tumour growth and angiogenesis. KIM-1 expression on RCC cells is associated with increased levels of transforming growth factor beta (TGF-β), which has been shown to promote metastatic invasion (Bostrom, Lindgren et al. 2013, Sabbiseti 2014). In contrast, a study previously published by our lab demonstrated that KIM-1 expression on TECs inhibits Gα$_{12}$, which consequently results in the inhibition of downstream RhoA – a small GTPase

involved in invasion and metastasis (Ismail, Zhang et al. 2016). We however have not examined the role of KIM-1 and $G\alpha_{12}$ in RCC cells. Therefore, the precise role that KIM-1 plays in RCC remains poorly understood.

1.4 Rationale, Objective, and Hypothesis

1.4.1 Rationale

RCC is the most common form of kidney cancer, and makes up over 90% of all cases (De, Otterstatter et al. 2014). Patients with stage IV metastatic RCC have a frighteningly low 5-year survival rate of only 8%, of whom comprise of over 30% of patients at the time of diagnosis (Canadian Cancer Society 2015). Current available therapies fall short due to the development of resistances and toxicities, compounded with suboptimal response rates in clinical trials (Massari, Santoni et al. 2015, Raman and Vaena 2015). Targeted therapies such as mTOR inhibitors, and VEGF inhibitors have been limited by resistance and toxicity (Su, Stamatakis et al. 2014), and immunotherapies such as PD-1/PD-L1 inhibitors have demonstrated limited response rates in clinical trials (Massari, Santoni et al. 2015). Surgery is often the most effective form of treatment in patients with non-metastatic RCC, but only offers palliation and symptom relief in patients with the metastatic form of the disease (de Vivar Chevez, Finke et al. 2014). There is hence an urgent need for novel therapeutic targets for the treatment of metastatic RCC.

In RCC, studies have found that KIM-1 is overexpressed in over 90% of RCC tumours, which includes the 2 most prevalent and aggressive forms of the disease: clear cell and papillary (Bonventre 2014, Zhang, Mashni et al. 2014). This overexpression is important since it is absent in healthy kidneys, and either absent or markedly reduced in patients that have undergone nephrectomy. The biological significance of this overexpression is still unclear; it is unknown whether KIM-1 overexpression *promotes* the disease, or if KIM-1 is overexpressed *because* of the disease.

The Cancer Genome Atlas (TCGA) is a publicly available cancer genomics program that has characterized the molecular profiles of over 20,000 primary cancers and profiled 33 types of cancers (National Cancer Institute 2006). We mined TCGA database in hopes of understanding how KIM-1 expression correlates with clinical outcome in patients. From

our unpublished data, we found that the high KIM-1 expressing patients had surprisingly greater overall survival compared with low KIM-1 expressing patients (Appendix A 1). Despite KIM-1 being absent in healthy kidneys, and it being overexpressed in the majority of RCC tumours, there appears to be an apparent protective effect in human patients.

There remains a vacuum in understanding on the role that KIM-1 plays in the metastasis of RCC in humans. KIM-1 appears to be a promising candidate to study and may lead to the development of novel therapeutic targets for the treatment of metastatic RCC. Given that metastasis is the most common cause of death in patients with RCC, and that KIM-1 expression is predictive of overall survival, KIM-1 may play a role in regulating metastasis in RCC. Determining whether KIM-1 plays a role in the development of metastatic RCC and elucidating the mechanisms behind its effects in RCC would be beneficial to understanding metastasis in the disease.

1.4.2 Objective and Hypothesis

The objective of this study was to determine the role that KIM-1 plays in the metastatic cascade of RCC and to elucidate the mechanism behind the action of KIM-1 and its downstream effectors. This study could ultimately help identify KIM-1 as a novel therapeutic target for the treatment of metastatic RCC.

We hypothesized that KIM-1 inhibits the metastatic potential of RCC cells. The specific aims of the work outlined in this thesis were; 1) To determine whether KIM-1 inhibits metastatic capabilities *in vitro*; 2) To determine whether KIM-1 inhibits invasion and metastasis *in vivo*; 3) To determine whether KIM-1-mediated inhibition of metastasis is dependent on adaptive immunity, and; 4) Elucidate genes that are differentially expressed between KIM-1$^+$ and KIM-1^{neg} cells. We predicted that; KIM-1 expression on RCC cells inhibits cancer cell invasion and metastasis both *in vitro* and *in vivo*; KIM-1-mediated inhibition of invasion and metastasis *in vivo* is independent of any contribution from the adaptive immune system, and; KIM-1 expression inhibits downstream effectors involved with invasion and metastasis.

Chapter 2

2   Materials and Methods

2.1   Generation of Stable Cell Lines

2.1.1   Plasmid Preparation and Transfection

Dr. Lawrence Kane (University of Pittsburgh, Pittsburgh, PA) generously provided the pCDEF3-mTim-1 (mKim-1) plasmid (Addgene plasmids # 49206; Cambridge, MA) and the parental pCDEF3 plasmid. DH5α competent cells transformed with either the pCDEF3-mKim-1 plasmid or pCDEF3 vector alone were grown overnight in LB media (1% w/v tryptone, 0.5% w/v yeast extract, 1% w/v NaCl) with 100 mg/ml ampicillin at 37° C with shaking. Plasmids were isolated using Geneaid midi plasmid kit (Geneaid Biotech Ltd., New Taipei City, Taiwan) following the manufacturer's protocol. Renca cells were plated in 6-well plates in complete medium and incubated until cells reached approximately 70% confluency. Renca cells stably expressing Kim-1 (Renca-pCDEF3-Kim-1) or pCDEF3 (Renca-pCDEF3) were generated by transfecting them with 2.5 μg of either pCDEF3-Kim-1 or pCDEF3 vector using 6 μl Lipofectamine® 2000 (ThermoFisher Scientific). After 24 h, the Renca cells were moved to a 15-cm plate and subjected to G418 selection (400 μg/ml) 48-h post-transfection. Renca cells were cultured continuously in the presence of G418 until non-transfected cells were completely killed. G418-resistant colonies were picked by aspirating medium, washing cells with 1x phosphate-buffered saline (PBS; 137 mM NaCl, 2.7 mM KCl, 4.3 mM Na2HOP4, 1.47 mM KH2PO4, pH 7.4) solution, and incubating cells with pre-cut pieces of filter paper soaked in 0.25% trypsin-EDTA (Invitrogen) for 5 minutes in a 37°C, 5% (v/v) CO2 incubator. Filter paper with attached cells were picked and grown in 24-well plates in full medium containing 400 μg/ml G418 until cells reached confluency. Individual colonies were then expanded, and Kim-1 expression was confirmed using western blot.

2.1.2   Stable Expression of Kim-1 Using Lentiviral Particles

Lentivirus ORF particles containing a vector with the murine Kim-1 gene, *Havcr1* and a puromycin resistance gene (MR203831L3V; Origene, Rockville, MD) were used to

transduce Renca cells (herein referred to as Kim-1$^+$ Renca). A control lentivirus ORF particle containing the same vector but lacking the Kim-1 transcript (PS100092V; Origene) was used as a control (Kim-1^{neg} Renca). The optimal concentration of lentiviral particles to use was determined based on testing various multiplicities of infection (MOIs), which is the number of transducing lentiviral particles per cell. To calculate the total transducing units (TU) needed; the total number of cells per well is multiplied by the desired MOI. Then, the total TU needed is divided by the titer of the virus purchased in TU/ml to give the total mL of lentiviral particles to be added to each well. Renca cells were seeded on a 24-well plate in full medium and incubated for 24 h when 75% confluency was reached. The medium was aspirated and replaced with full medium containing 8 μg/mL of polybrene (Santa Cruz Biotechnology) and the appropriate number of lentiviral particles (either control particles or particles containing the Kim-1 transcript). After 24 h, the medium was aspirated and replaced with full medium. 72 h post-transduction, stable cell lines were selected for using medium supplemented with puromycin. Medium was aspirated and replaced with full medium containing 2 μg/ml of puromycin every 2–3 days for two weeks. After two weeks, cells transduced with Kim-1 ORF lentiviral particles were screened for Kim-1 expression via western blot and PCR.

2.1.3 shRNA Knock-down of Endogenous KIM-1 Using Lentiviral Particles

Lentiviral particles containing three human KIM-1-specific constructs encoding shRNA (sc-61691; Santa Cruz) were used to knockdown KIM-1 in the 769-P and 786-O cell line (herein referred to as 769-P-/786-O-shKIM-1). Control transduction was done using control scrambled shRNA lentiviral particles (769-P-/786-O-shcontrol) (sc-108080; Santa Cruz). 769-P/786-O cells were plated on a 12-well plate in full medium and incubated for 24 h until 75% confluency was reached. The medium was aspirated and replaced with 1 mL total volume of full medium containing 8 μg/mL of polybrene (Santa Cruz Biotechnology) and 25 μL of lentiviral particles (either shKIM-1 or shcontrol lentiviral particles). After 24 h, the medium containing polybrene and lentiviral particles was aspirated and replaced with complete medium. 72-h post-transduction, stable cell lines expressing the respective shRNA were isolated via selection with puromycin. Medium was

aspirated and replaced with full medium containing 4 µg/ml of puromycin every 2–3 days for two weeks. After two weeks, knockdown of KIM-1 in 769-P and 786-O cells was confirmed via western blot and PCR.

2.2 Western Blot

Confluent monolayers of the respective cells (Renca, 769-P and 786-O) were lysed with ice cold 4% sodium dodecyl sulfate (SDS) and centrifuged at 15,000 x g for 10 minutes. The supernatants were collected for western blot analysis. Protein concentrations were determined using the Pierce BCA Protein Assay Kit (ThermoFisher Scientific) and samples were prepared such that they contained 50 µg of total protein. Proteins were separated by SDS-PAGE and transferred to a polyvinylidene difluoride (PVDF) membrane (EMD Millipore, Billerica, MA). Membranes were blocked with blocking buffer (Tris-buffered saline, 0.1 % Tween-20 (ThermoFisher Scientific), and 5% non-fat dried milk (Carnation)) for 1 h. Membranes were then incubated overnight at 4°C with primary antibodies: extracellular domain of human KIM-1 (AKG; Dr. Bonventre, Harvard Medical School, Cambridge, MA), extracellular domain of mouse Kim-1 (AF1817; R&D systems, Minneapolis, MN), or GAPDH (6C5; Santa Cruz Biotechnology). Membranes were washed and incubated with the appropriate horseradish peroxidase-conjugated secondary antibody (dilution 1:30000; Jackson ImmunoResearch Laboratories, West Grove, PA) for 1 h at room temperature in blocking buffer. Proteins were visualized using Luminata Forte Western HRP Substrate (EMD Millipore) and developed using the FluorChem M system (ProteinSimple, San Jose, CA).

2.3 RNA Extraction and cDNA Synthesis

Cell and tissue samples were collected in TriPure isolation reagent (Roche Diagnostic, Basel, Switzerland). 200 µL of chloroform per 1 mL of TriPure reagent used was added to samples and then mixed vigorously. The samples were incubated for 10 minutes at room temperature and then centrifuged at 12,000 x g for 20 minutes at 4°C. The aqueous layer was carefully recovered in a fresh tube and an equal volume of isopropanol was added to the aqueous layer for precipitation. The mixture was vortexed briefly, incubated at room temperature for 10 minutes, and then centrifuged at $12,000 \times g$ for 10 minutes at 4°C. The

supernatant was removed from the tube and the pellet was washed with 70% ethanol, and subjected to centrifugation at 7,500 x g for 5 minutes at 4°C. After removal of the supernatant, the pellet was resuspended in DEPC-treated water and quantified with spectrophotometry (260 and 280 nm; MultiskanTM GO Microplate Spectrophotometer; ThermoFisher Scientific). 1 μg of total RNA and 4 μL of qSCRIPT cDNA SuperMix (Quanta Biosciences, Gaithersburg, MD) were used to generate cDNA using the MyCyclerTM thermal cycler (Bio-Rad, Hercules, CA).

2.3.1   Real Time-PCR (RT-PCR)

RT-PCR was performed using the StepOnePlus Real-Time PCR System (Applied Biosystems, Waltham, MA) and SYBR Green detection (ThermoFisher Scientific). The reaction mixture had a total reaction volume of 20 μL, which consisted of 10 μL of SYBR Green Master Mix, 0.2 μL of each 10 μM forward and reverse primer for the gene of interest, 4.6 μL of DEPC treated water, and 5 μL of cDNA diluted in DEPC-treated water at a ratio of 1:10. Primers for KIM-1 and GAPDH are shown in Table 1 (Integrated DNA Technologies, Coralville, IA). Normalization of the target gene was performed to GAPDH to compensate for inter-PCR variations. Relative gene expression was calculated using the 2-ΔΔCt method.

2.3.2   Standard PCR

The reaction mixture had a total volume of 25 μL, which consisted of cDNA, DEPC treated water, 200 μM of forward and reverse primer for the gene of interest, 2 U/rxn of Taq DNA polymerase (Invitrogen), 1.5 mM MgCl2 (Invitrogen), 0.2 mM of dNTP mix (Clontech Laboratories, Mountain View, CA), and 1x PCR Reaction Buffer (Invitrogen). Primers for KIM-1 and GAPDH are shown in Table 1 (Integrated DNA Technologies). Amplicons were resolved using a 1% agarose gel via gel electrophoresis in 1x TBE buffer (Tris/borate/EDTA; 0.09 M Tris (hydroxymethyl) Aminomethane, 0.09 M Boric Acid, 0.1 mM EDTA). Amplicons were visualized with ethidium bromide and UV light using the FluorChem M system (ProteinSimple). Target genes were normalized to GAPDH.

2.1   Cell Culture

The murine RCC line, Renca, was purchased from ATCC (CRL-2947). Cells were maintained according to ATCC recommendations. Cells were cultured in RPMI-1640 medium, supplemented with L-glutamine and 25 mM HEPES (Lonza, Walkersville, MD), 10% fetal bovine serum (FBS; Invitrogen, Carlsbad, CA), 2 mM L-glutamine (ThermoFisher Scientific, Waltham, MA), 1 mM sodium pyruvate (ThermoFisher Scientific), 0.1 mM non-essential amino acids (ThermoFisher Scientific), and 5% penicillin streptomycin (PS; Invitrogen). Stable Renca cell lines were maintained with 2 mM puromycin dihydrochloride (Sigma-Aldrich, St. Louis, MO). The human RCC cell lines, 786-O and 769-P, were purchased from ATCC (CRL-1932). Cells were cultured in DMEM medium, supplemented with L-glutamine, sodium pyruvate, and phenol red (Wisent Bioproducts, Saint-Jean Baptiste, QC), 10% FBS, and 5% PS. Stable 786-O cell lines were maintained with geneticin sulfate (G418; Santa Cruz Biotechnology, Santa Cruz, CA). All cells were maintained in a $37^{\mathbf{o}}$ C, 5% (v/v) CO_2 incubator.

2.2   Migration and Invasion Assay

Cell migration and invasion were used as surrogates for metastatic potential of RCC cells *in vitro*. Transswell culture plates with 8.0-µm-pore-size polycarbonate membrane filter inserts with 6.5 mm diameter (Corning, NY) were used to perform migration and invasion assays. Plate wells were filled with 800 µL of serum-free media (SFM) or complete media with 10% FBS (Renca in RPMI; 786-O in DMEM). Renca cells were cultured to a confluency of ~80% and resuspended in SFM at a concentration of $2x10^5$ cells/mL. 786-O cells were cultured to 100% confluency, starved for 24h prior to collection, and resuspended in SFM at a concentration of $1x10^5$ cells/mL. 200 µL of cells were seeded in the Transswell insert and plates were incubated for 24 h in a $37^{\mathbf{o}}$ C, 5% (v/v) CO_2 incubator. For invasion assays, Transswell inserts were coated with 200 µL of Matrigel (1:100 dilution in SFM; BD Biosciences, NJ) 24 h prior to seeding of cells. After incubation, media was aspirated from the inserts and wells, and lightly blotted dry using cotton swabs. Subsequently, 1 mL of cold methanol was added to each well, and inserts were replaced and incubated at RT for 5 minutes to fix the cells. Methanol was aspirated, and 1 mL of eosin dye (Sigma-Aldrich) was added to each well and incubated at RT for 5 minutes. This

process was repeated using a secondary toluidine blue dye (Sigma-Aldrich). Wells were then washed twice at RT with 2 mL of distilled water for 5 minutes each. Inserts were then removed and placed upside down to dry on benchtop for 30 minutes. Using a scalpel blade, insert membranes were carefully cut out, fixed on a glass slide and allowed to dry overnight at RT. Light microscopy was used to quantify the migrated and invaded cells. All assays were performed in triplicate.

2.3 Extravasation Efficiency Assay in the CAM of Chick Embryos

Methods and protocols for CAM extravasation model was conducted by Marie Sarabusky as previously described in the laboratory of Dr. Hon Leong (then) at the Lawson Health Research Institute (Kim, Williams et al. 2016). Renca and 769-P cells were plated on cell culture flasks and grown until 80% confluency was obtained. Medium was aspirated, cells were washed with 1x PBS, and then cells were incubated for 5 minutes with 0.25% trypsin-EDTA in a 37°C, 5% (v/v) CO_2 incubator. Cells were centrifuged for 5 minutes at 500 x g, the supernatant was aspirated, and cells were resuspended in 1 mL of 1x PBS. Cells were fluorescently labeled using 1 µL of CellTracker dye (ThermoFisher Scientific) and incubated on ice for 5 minutes. Cells were centrifuged for 5 minutes at 500 x g and the supernatant was aspirated. A day 13 embryo was placed under a dissecting scope with white light illumination in order to visualize the veins in the CAM. The cell suspension was drawn up into a microinjector and $1x10^5$ KIM-1$^+$ or KIM-1^{neg} cells were injected into the vein of the CAM. Following the injection, two filter square windows were placed on the surface of the embryo at sites away from the injection site. A wide-field fluorescent microscope at 10x objective was used to count and record all the cells within each square window immediately after injection. All cells at this time point (T = 0 h) are intravascular. 24 h later, the fluorescent microscope was used again to count and record the number of intravascular and extravascular cells (T = 24 h). The extravasation efficiency was determined by dividing the number of extravasated cells at T = 24 h by the number of intravascular cells at T = 0 h in each of the square windows (Kim, Williams et al. 2016). The mean extravasation efficiency for all foil windows on each embryo was then determined. To obtain intravital images of intravascular and extravasated cells, the CAM

was additionally injected with lectin-DyLight 649 (Vector Laboratories, Burlington, ON) and Dextran-Alexa 555 (ThermoFisher Scientific) and imaged using a confocal microscope (Olympus, Tokyo, Japan) with the 60x objective at T = 0 h and T = 24 h.

2.4   Mice

Female *wild-type* (WT) BALB/c mice were purchased from Charles River Laboratory (Wilmington, MA) and maintained in the pathogen-free animal facility at Western University. Mice were kept in standard shoebox cages with access to pellet food and bottled tap water in rooms maintained at constant temperatures (22° C) with 12-h light/12-h dark cycles. Immune-deficient C129-Rag (Rag1$^{-/-}$) mice were purchased from Jackson Laboratory (Bar Harbor, ME) and maintained in the pathogen-free barrier facility at Western University. Mice were kept in pathogen-filtered shoebox cages with access to pellet food and water through a filtered nozzle, and maintained in similar room conditions. Experimental mice were monitored every 2 days for physiological and behaviour changes. All mice were euthanized using CO_2 chambers, and post-mortem procedures were conducted as described. All animal protocols (2010-230, later renewed 2018-147) and experiments were approved by Western University's Animal Use Subcommittee in compliance with the guidelines set by the Canadian Council of Animal Care.

2.5   Experimental Metastasis Model

2.5.1   Intravenous Injection of RCC cells

To study experimental metastasis of RCC cells into the lungs, 6-10-week-old female WT BALB/c mice were injected with Renca cells via lateral tail vein. Renca cells were cultured in cell culture flasks up to a confluency of 80%. Media was aspirated, and cells were washed with 5 mL of cold 1x PBS, and then incubated with 10 mL of cold 1x PBS at room temperature (RT) for 10 minutes. PBS was aspirated and replaced with 3 mL of 0.25% trypsin-EDTA (Wisent Bioproducts) for 5 minutes in a 37° C, 5% (v/v) CO_2 incubator. Cells were then flushed with 6 mL of complete RPMI-1640 media to dislodge adherent cells, which were then collected and centrifuged at 500 x g for 5 minutes, and the supernatant was subsequently aspirated. Cells were counted using trypan blue and a hemocytometer, and viable cells were then resuspended at a concentration of 2.5×10^6

cells/mL in sterile 1x PBS. Mice were restrained using a cylindrical mouse restrainer (Stoelting, Wood Dale, IL) and injected with 200 µL (5 x 10^5 cells) of Renca cells via the lateral tail vein, using a ½ inch 28-gauge insulin syringe (Becton Dickinson, Franklin Lakes, NJ). Mice were monitored after 24 h, and then every 2 days until day 17, at which point, they were euthanized using a CO_2 chamber. To study whether KIM-1-mediated inhibition of metastasis is dependent on adaptive immunity, Renca or 786-O cells were instead injected into the tail veins of immune-deficient BALB/c (Rag1$^{-/-}$) mice in the same manner as described above.

2.5.2 Staining of Lungs and Visualization of Metastatic Nodules

We used a modified version of the protocol described by Zimmerman et al. (Zimmerman, Hu et al. 2010) to stain the lungs of mice injected either intravenously or orthotopically with RCC cells and for visualization of metastatic nodules. Euthanized mice were pinned down on their dorsal side, and their chest cavity was opened up along the sternum using scissors to expose the lungs and trachea. The trachea was clamped down at the highest possible point with tweezers, and 2 mL of 15% India black ink (diluted in distilled water) was slowly injected into the trachea below the clamp, expanding the lungs and turning them black. Lungs were excised, detached from the heart and thymus, and placed in a beaker of distilled water for 5 minutes to wash off excess ink. The lungs were then transferred to a 15 mL Falcon tube (ThermoFisher Scientific) containing 5 mL of Fekete's solution (Appendix A 2) to expose the metastatic tumour tissue as white nodules. Lungs were incubated overnight at 4° C before being washed with 1x PBS and metastases counted under a low power light microscope.

2.6 Spontaneous Metastasis Model

To study the spontaneous metastasis of RCC cells to the lungs, Renca cells were orthotopically injected into kidney capsules of 10-14-week-old female WT BALB/c mice. Mice were first anesthetized with Ketamine/Xylazine (100 mg/kg, 16 mg/kg), and given slow-release buprenorphine (1 mg/kg) for pain control. The drugs were injected subcutaneously according to institutional guidelines. Injection site (left flank) was shaved and prepared with 5% povidone-iodine antiseptic. An incision (~1.5-2 cm) was carefully

made using sterile scalpel and scissors to not penetrate the peritoneum. The dermis layer and peritoneum were then carefully separated. The kidney was identified underneath the spleen and held in place using forceps. Carefully, 30 µL of cell suspension (2×10^5 cells in a 1:1 ratio with Matrigel) was injected into the subcapsular space of the kidney and held in place for a minute while a heat lamp was placed overhead to solidify the Matrigel. The incision was closed, and the animal was returned to its cage and monitored until it recovered to parameters set by institutional guidelines. Once the injections were completed, the mice were monitored after 24, 48, and 72 h, and then every 2 days after until day 17. Mice were then sacrificed, and lungs were stained and collected as described previously.

2.7 RNA Sequencing

RNA sequencing was performed by London Genomics Centre under the guidance of Dr. Rob Hegele at the Robarts Research Institute (Western University). RNA extraction and cDNA library synthesis were performed as described above with Kim-1$^+$ and Kim-1^{neg} Renca cells. Adapter sequences specific to the Illumina sequencing platform was used. Libraries were sequenced using the Illumina NextSeq 500 sequencer (Illumina Inc., San Diego, CA). A bioinformatic pipeline was built using the Partek Flow software (Partek Inc., St. Louis, MO) to compare differences in gene expression between Kim-1$^+$ and Kim-1^{neg} Renca cells. A heat map was generated by changing parameters to only include genes with significant differences with $p < 0.05$ and exclude fold-changes between -1.5 and 1.5 (Figure 9). Gene pathway and gene set enrichment were performed to determine biological pathways and specific genes relevant to invasion and metastasis. The same stringency values used to generate the heat map were applied. The pathways and genes are displayed in Table 2 and 3.

2.8 Statistical Analysis

Differences in means between KIM-1$^+$ and KIM-1^{neg} groups for all results were analyzed using unpaired two-tailed t-tests. Statistical significance was defined as: *, $p < 0.05$; **, $p < 0.01$; ***, $p < 0.001$. Data was represented as mean ± SEM. Statistical analyses were performed using the GraphPad Prism, version 8 software.

Chapter 3

3   Results

3.1   Renca cells expressing Kim-1 exhibited decreased metastatic potential *in vitro*

To understand the metastatic potential of Renca cells *in vitro*, Transwell migration and invasion assays were performed (Figure 3). Renca cells were seeded in the Transwell inserts, and SFM or complete media (RPMI with 10% FBS) was loaded (underneath) into the plate wells. For invasion assays, the Transwell insert membranes were coated with Matrigel prior to cell seeding. Kim-1^{+} Renca cells showed significantly reduced migratory capability compared with Kim-1^{neg} Renca cells in both the SFM group (22.67 vs. 40.33), and the 10% group (51 vs. 76.67), respectively (n = 3; SFM, p = 0.0049; 10%, p = 0.0307) (Figure 3A). Kim-1^{+} Renca cells also exhibited significantly fewer invading cells compared with Kim-1^{neg} Renca cells, in the SFM group (35.33 vs 50.33), and in the 10% group (34 vs. 49.33), respectively (n = 3; SFM, p = 0.0006; 10%, p = 0.0005) (Figure 3B). Together, these data demonstrate that Kim-1 expression inhibits the migration and invasion of Renca cells *in vitro*.

A

B

C

D
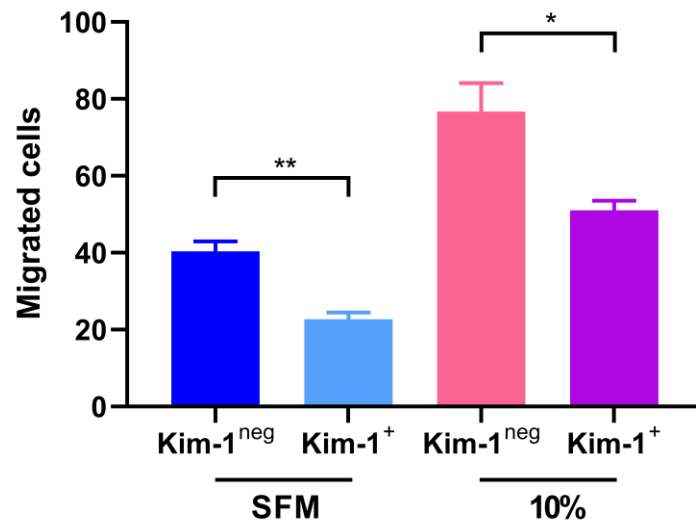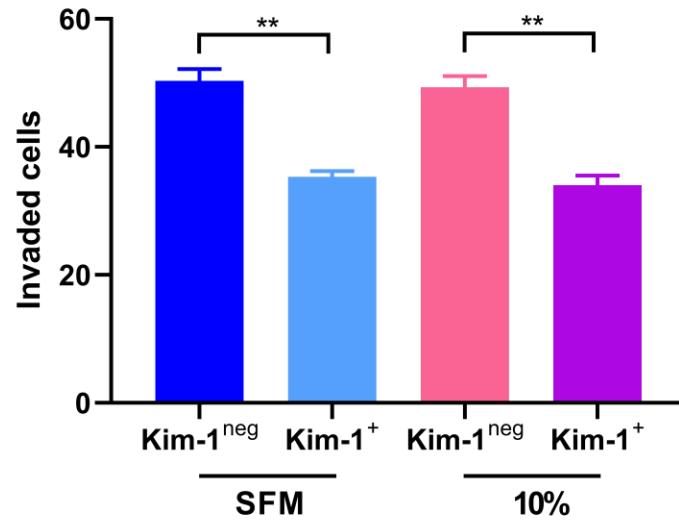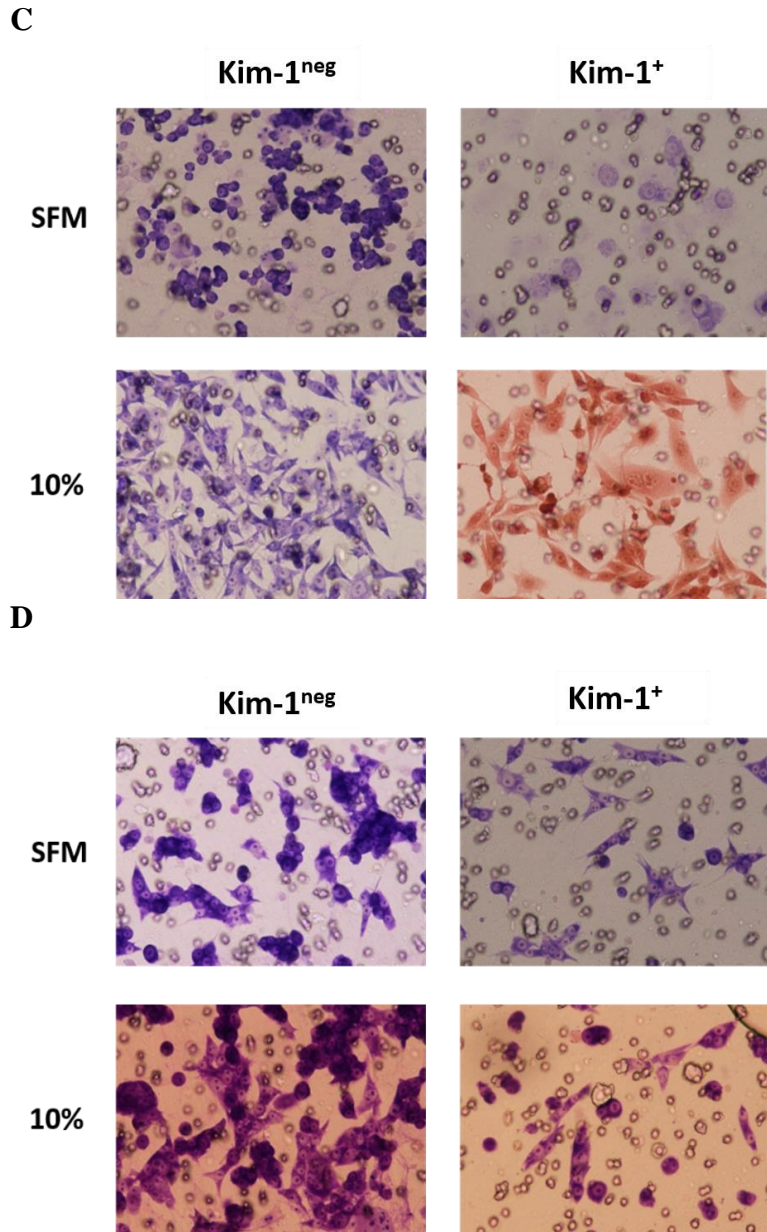
Figure 3. Transwell migration and invasion assay of Kim-1$^+$ and Kim-1^{neg} Renca cells.

(A) Migration assay of Kim-1$^+$ and Kim-1^{neg} Renca cells (n=3) **(B)** Invasion assay of Kim-1$^+$ and Kim-1^{neg} Renca cells (n=3). **(C)** Images of migration assay Transwell insert membranes (10X) **(D)** Images of invasion assay Transwell insert membranes (10X). 2 x 10^5 Renca cells were seeded in serum-free RPMI media in Transwell inserts on top of wells filled with serum-free or complete RPMI media supplemented with 10% FBS. Plates were incubated at 37° C for 24h. Transwell insert membranes for invasion assay were coated with Matrigel 12h prior to seeding. Data is represented as mean number of cells $\pm$ SEM (**A**; SFM, p = 0.0049; 10%, p = 0.0307. **B**; SFM, p = 0.0019; 10%, p = 0.0028, Unpaired two-tailed t-test). SFM, serum-free media; 10%, complete RPMI media supplemented with 10% FBS.

3.2 KIM-1 expression on 786-O cells inhibits invasion *in vitro*

To understand the metastatic potential of human RCC (786-O) cells *in vitro*, Transwell migration and invasion assays were performed (Figure 4). 786-O cells were seeded in the Transwell insert, and SFM or complete media (DMEM with 10% FBS) was loaded into the plate wells. No significant differences were observed between 786-O-shcontrol and 786-O-shKIM-1 cells in the migration assay (Figure 4A). 786-O-shcontrol cells displayed significantly fewer number of invaded cells compared with 786-O-shKIM-1 cell in the SFM group (42 vs. 98; p = 0.0006) and in the 10% group (22 vs. 36.7; p = 0.0396) (Figure 4B). Together, these data indicate that KIM-1 expression inhibits the invasion of 786-O cells *in vitro*.

A

B

C

D
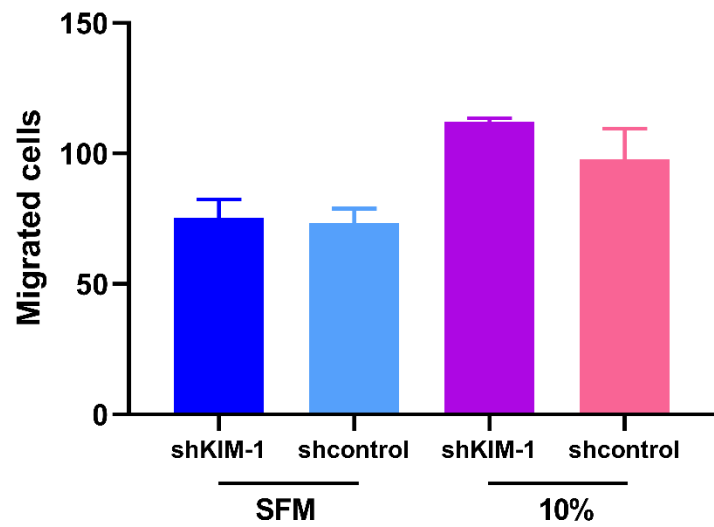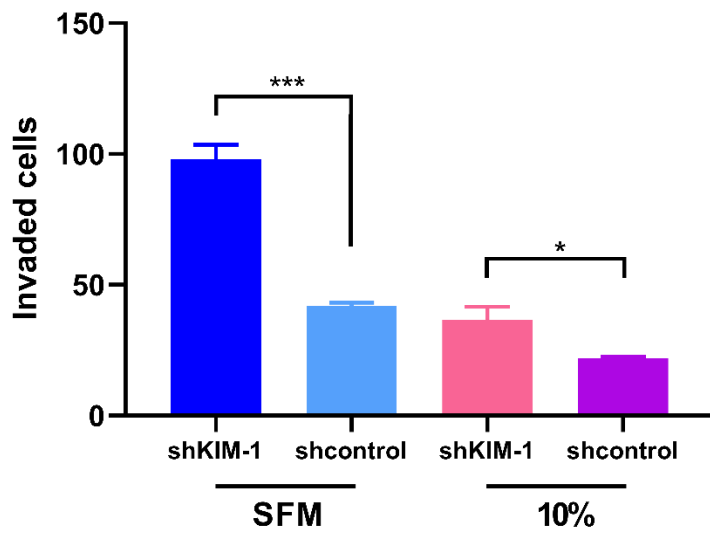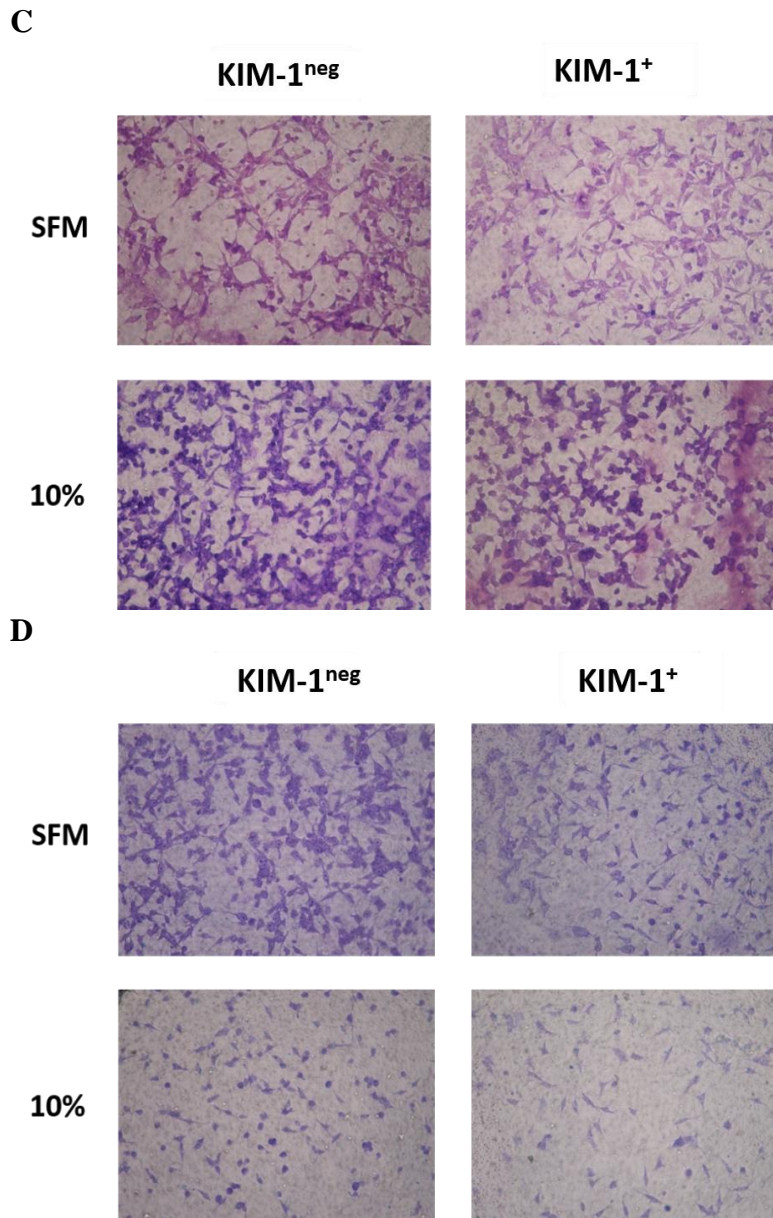
Figure 4. Transwell migration and invasion assay of 786-O-shcontrol and 786-O-shKIM-1 cells.

 (A) Migration assay of 786-O-shcontrol (KIM-1$^+$) and 786-O-shKIM-1 (KIM-1^{neg}) cells (n=3) (B) Invasion assay of 786-O-shcontrol (KIM-1$^+$) and 786-O-shKIM-1 (KIM-1^{neg}) cells (n=3). (C) Images of migration assay Transwell insert membranes. (D) Images of invasion assay Transwell insert membranes. 1×10^5 786-O cells were seeded in serum-free DMEM media in Transwell inserts on top of wells filled with serum-free or complete DMEM media supplemented with 10% FBS. Plates were incubated at 37° C for 24h. Transwell insert membranes for invasion assay were coated with Matrigel 12h prior to seeding. Data is represented as mean number of cells $\pm$ SEM (B; SFM, p = 0.0006; 10%, p = 0.0396, Unpaired two-tailed t-test). SFM, serum-free media; 10%, complete DMEM media supplemented with 10% FBS.

3.3 Kim-1 expression decreases cancer cell extravasation efficiency of murine Renca cells

To determine the ability of cancer cells to extravasate out of capillaries, fluorescently labeled Renca cells were injected into the vein in the CAM of a day 13 chick embryo. An image of a chick embryo on day 13 reveals the tumor cell injection site and two filter square windows, in which cells were counted at $T = 0$ h and $T = 24$ h using a fluorescent microscope (Figure 5A). Figure 5B contains a typical confocal image of the fluorescently labeled components of the vasculature (endothelial walls and vessel lumen space) with Renca cells labeled in green to depict intravascular and extravasated cells. Intravascular cells had an irregular morphology and were retained within the blood vessel (top panel), whereas extravasated cells had a rounded morphology and appeared to be present in the extracellular stroma (lower panel) (Figure 5B). Kim-1$^+$ Renca cells had an extravasation efficiency of 47.78% which was significantly decreased compared to Kim-1^{neg} Renca control cells, which had an extravasation efficiency of 60.73% ($n = 6$; $p < 0.05$) (Figure 5C). Overall, Kim-1 expression appears to decrease extravasation efficiency of the murine Renca cell line.

3.4 KIM-1 expression decreases cancer cell extravasation efficiency of human 769-P cells

Fluorescently labeled human RCC (769-P) cells stably expressing shRNA targeting KIM-1 or control shRNA were injected into the vein in the CAM of a day 13 chick embryo. 769-P-shcontrol cells had an extravasation efficiency of 30.08% which was significantly decreased compared to 769-P-shKIM-1 cells, which had an extravasation efficiency of 47.94% ($n = 6$; $p < 0.0001$) (Figure 5C). These data appear to indicate KIM-1 expression decreases extravasation efficiency of human 786-O cells.

A

B

C
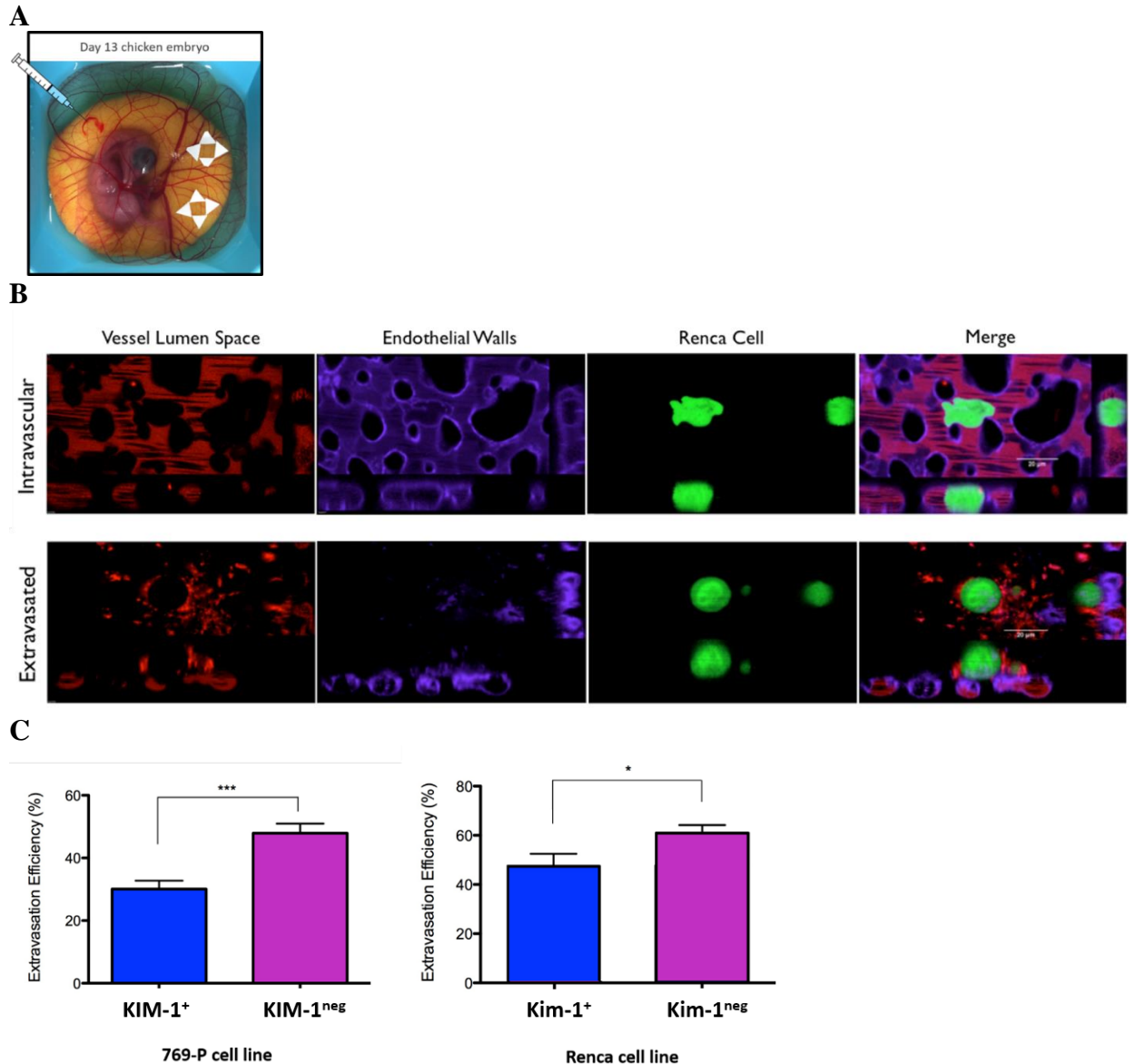
Figure 5. Chick chorioallantoic membrane (CAM) extravasation assay of 769-P and Renca cells.

(A) Image of chick embryo with representative location of tumour cell injections (needle) and filter square windows (white arrows). (B) CAMs used for confocal imaging were injected with fluorescent dyes to label the endothelial walls (purple) and the vessel lumen space (red), in addition to the fluorescently labeled cells (green). (C) 0.5×10^5 769-P (shcontrol/KIM-1$^+$ and shKIM-1/KIM-1^{neg}) and Renca (Kim-1$^+$ and Kim-1^{neg}) cells were injected into the vein in the CAM of a day 13 chick embryo (n = 6/ group). Two filter square windows were placed at sites on the CAM that were away from the injection site. Fluorescent cells were counted in the windows at T = 0 h and T = 24 h using a fluorescent microscope. Scale bar is 20 μm. Data is represented as mean of extravasation efficiency in percentage per group ± SEM (769-P, $p < 0.001$; Renca cells, $p < 0.05$, Unpaired two-tailed t-test). CAM, chorioallantoic membrane. *Methods and data adapted from Marie Sarabusky.

3.5 KIM-1 expression on Renca cells inhibits metastasis in an *in vivo* experimental metastasis model

To investigate the role of Kim-1 expression in the metastasis of Renca cells, we injected 5 x 10^5 Kim-1$^+$ Renca or Kim-1^{neg} Renca cells intravenously via the tail vein into 6-10-week-old female WT BALB/c mice. In this experimental metastasis model, intravenously injected cancer cells invaded the lung tissue and developed metastatic nodules (Gomez-Cuadrado, Tracey et al. 2017). Mice were sacrificed after 17 days (or if moribund), and their lungs were excised for examination of metastatic nodules following staining with 15% India black ink and Fekete's solution. Mice injected with Kim-1$^+$ Renca cells developed significantly fewer lung nodules compared to mice injected with Kim-1^{neg} Renca cells (n = 5; 256.6 vs. 429.4, p = 0.0226) (Figure 6). These data demonstrate that Kim-1-expressing Renca cells inhibit the development of lung metastases in an experimental metastasis model.
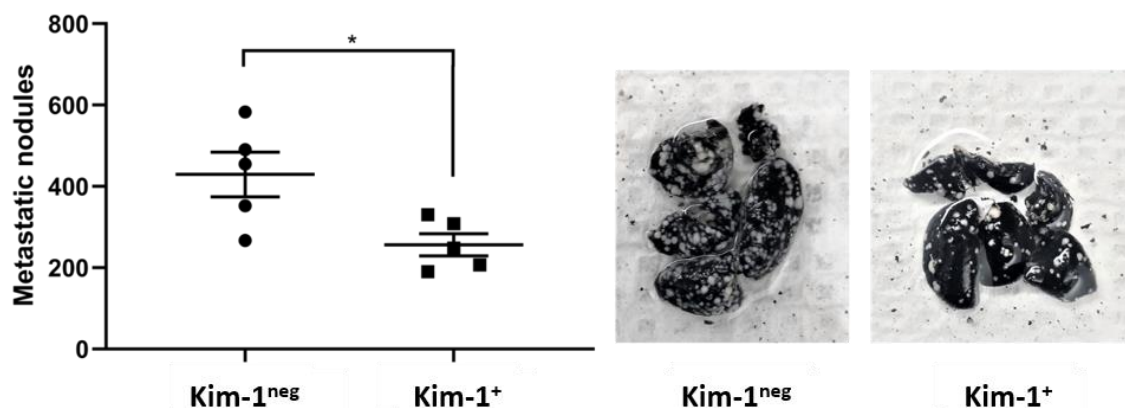
Figure 6. Kim-1 expression on Renca cells decreases experimental lung metastases in WT BALB/c mice

Approximately 5 x 10^5 Renca (Kim-1$^+$ and Kim-1^{neg}) cells were injected into 6-10-week-old female WT BALB/c mice via lateral tail vein (n = 5/ group). Mice were sacrificed in CO_2 chambers after 17 days. Lungs were removed, stained with 15% India black ink and counterstained with Fekete's solution to visualize metastatic tumour tissue. Data is represented as mean number of metastatic nodules ± SEM (p = 0.0226, Unpaired two-tailed test). WT, wild-type.

3.6   Kim-1 expression does not alter the metastatic potential of Renca cells in an *in vivo* spontaneous metastasis model

We injected 2 x 10^5 Kim-1$^+$ Renca or Kim-1^{neg} Renca cells orthotopically into the subcapsular space of the kidney of 8-12-week-old female WT BALB/c mice to investigate the effect of Kim-1 expression on Renca cell metastasis in a clinically relevant spontaneous metastasis model. No statistically significant differences were found between Kim-1$^+$ and Kim-1^{neg} cells at day 17 (Figure 7). The majority of injections yielded < 12 metastatic nodules, therefore, meaningful results could not be determined.
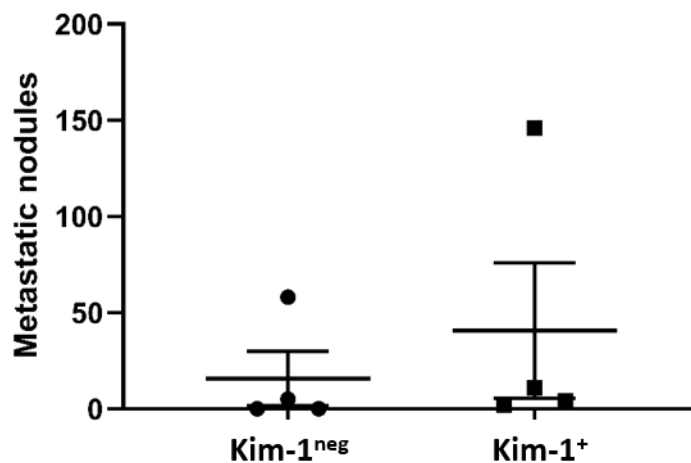
Figure 7. Kim-1 expression on Renca cells has no effect on the development of spontaneous lung metastases.

Approximately 2 x 10^5 Renca (Kim-1$^+$ and Kim-1^{neg}) cells were injected into the subcapsular space of the kidney of 8-12-week-old female WT BALB/c mice (n = 4/ group). Mice were sacrificed in CO_2 chambers after 17 days. Lungs were removed, stained with 15% India black ink and counterstained with Fekete's solution to visualize metastatic tumour tissue. Data is represented as mean number of metastatic nodules ± SEM. WT, wild-type.

3.7 Kim-1 expression on Renca cells inhibits metastasis *in vivo* independent of adaptive immunity

To determine whether the observed Kim-1-mediated inhibition of metastasis was dependent on the adaptive immune system, we repeated the above described experimental metastasis model using immune-deficient BALB/c (Rag1$^{-/-}$) mice as hosts instead of immune competent (WT) BALB/c mice. As described previously, 5 x 10^5 Renca cells were injected via the lateral tail vein of Rag1-deficient BALB/c mice. Mice injected with Kim-1$^+$ Renca cells developed significantly fewer metastatic nodules than mice injected with Kim-1^{neg} Renca cells (n = 5; 33.2 vs. 135.4, p = 0.036) (Figure 8A). These data show that Kim-1 decreases metastasis to the lungs in Renca cells independent of adaptive immunity.

3.8 KIM-1 expression on 786-O cells inhibits metastasis *in vivo* independent of adaptive immunity

To study the effect of KIM-1 expression on the metastasis of human cells, the above experiment was repeated with 786-O cells rather than Renca cells. Mice injected with 786-O-shcontrol cells developed significantly fewer metastatic nodules than mice injected with 786-O-shKIM-1 cells (n = 4 & 5; 130.6 vs. 339.3, p = 0.0013) (Figure 8B). Overall, these data indicate that KIM-1 expression in 786-O cells inhibits metastasis independent of the adaptive immune system.

A

B
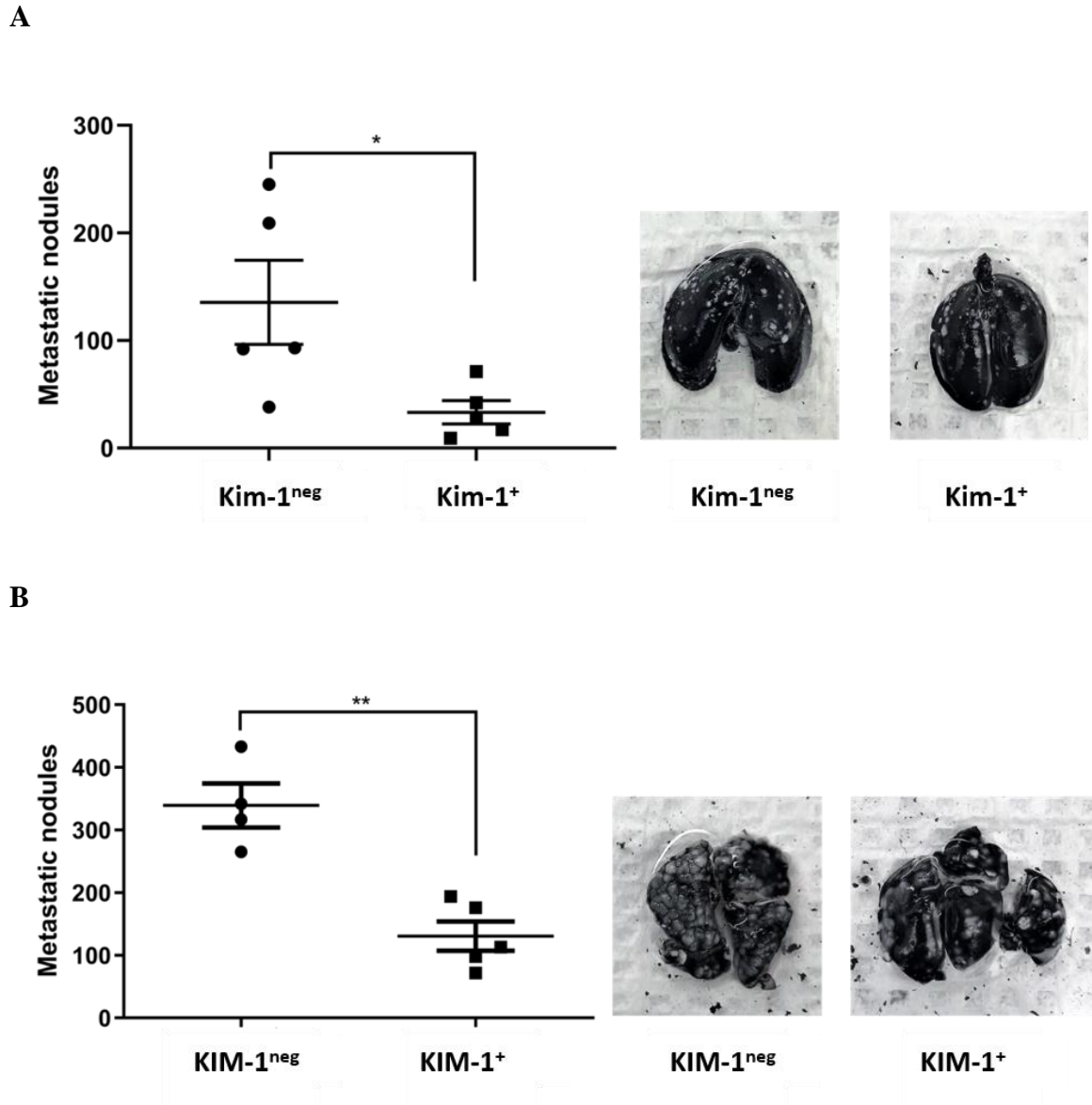
Figure 8. KIM-1 expression on Renca and 786-O cells decreases experimental lung metastases in Rag1-deficient mice

(A) Lung metastatic nodules from mice injected with Renca cells (n = 5). **(B)** Lung metastatic nodules from mice injected with 786-O cells (n = 4 & 5). 5 x 10^5 Renca (Kim-1^+ and Kim-1^{neg}) and 786-O (KIM-1^+ and KIM-1^{neg}) cells were injected into 6-10-week-old female immune-deficient Rag1$^{-/-}$ mice via lateral tail vein. Mice were sacrificed in CO_2 chambers after 17 days. Lungs were removed, stained with 15% India black ink and counterstained with Fekete's solution to visualize metastatic tumour tissue. Data is represented as mean number of metastatic nodules ± SEM (Renca, p = 0.036; 786-O, p = 0.0013, Unpaired two-tailed test).

3.9 RNA-sequencing of Renca cell lines to elucidate the mechanism of KIM-1-dependent inhibition of metastasis

In an attempt to identify a putative mechanism to explain how KIM-1 may be inhibiting metastasis in RCC cells, we performed RNA-sequencing to study the differential expressions of genes and gene pathways between Kim-1$^+$ Renca or Kim-1^{neg} Renca cells (Figure 9). Analysis of the RNA-seq data using broad pathway filtration techniques helped determine gene pathways which displayed significant differences between the two cell lines (Table 2). Stringency values were set to only include pathways with a p-value < 0.05. When analyzing the data for differences in specific genes between Kim-1$^+$ Renca or Kim-1^{neg} Renca cell lines, we determined a list of genes and the fold-change differences of Kim-1$^+$ cells relative to Kim-1^{neg} cells (Table 3). The stringency values were set to only include p-values < 0.05 and exclude fold-changes between -1.5 to +1.5. The highlighted pathway and gene in each table were scrutinized further and found to possess functions relevant to invasion and metastasis.
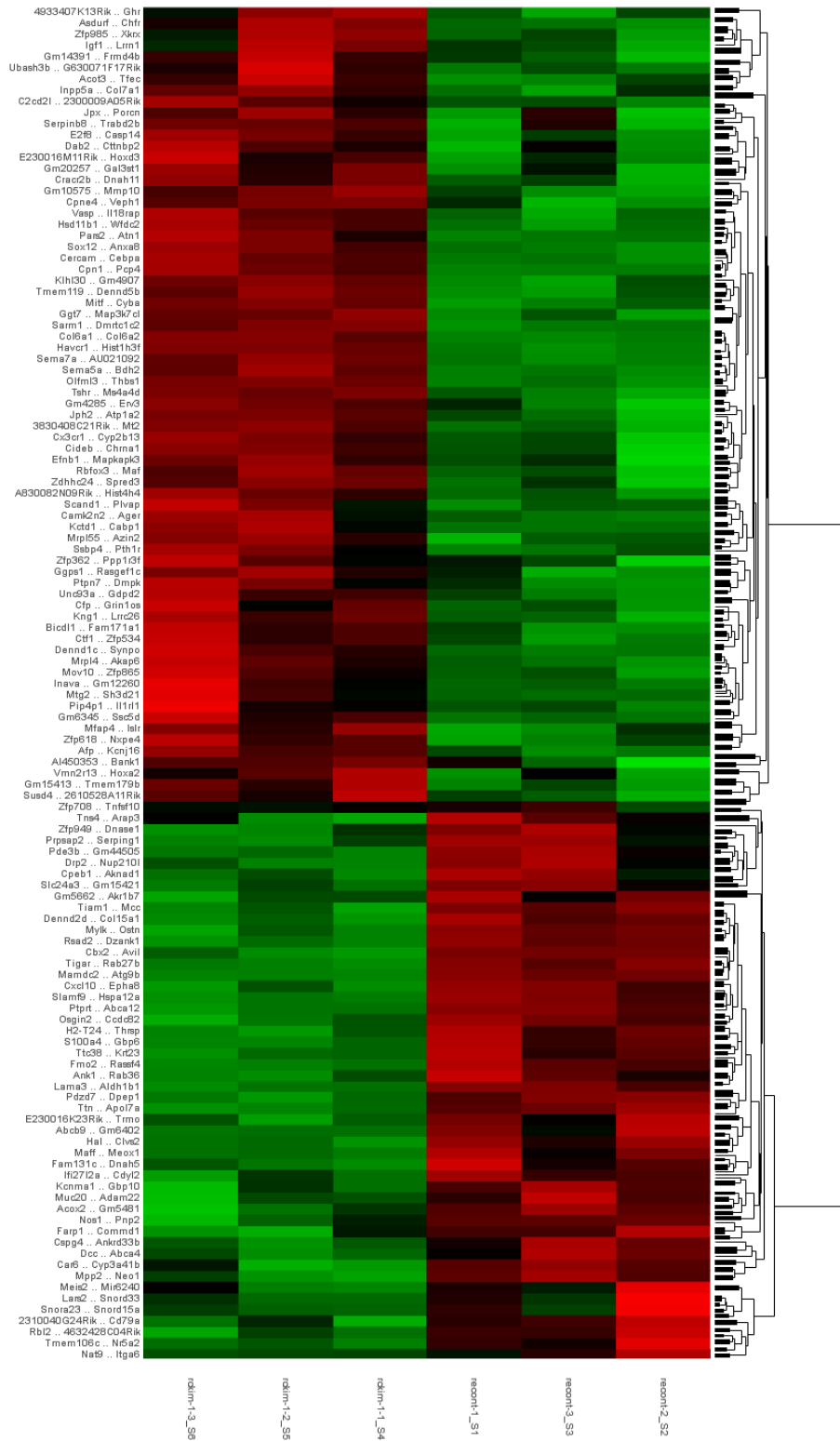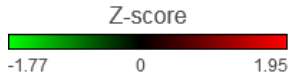
Figure 9. Heatmap of genes upregulated or downregulated by Kim-1 expression in Renca cells.

Heatmap of genes differentially expressed between Kim-1$^+$ and Kim-1^{neg} Renca cells generated through RNA sequencing. Only genes with significant differences ($p < 0.05$) are shown. Genes with fold-changes between -1.5 and +1.5 were excluded. Gene names are aligned along the left and gene clustering is shown on the right. Sample names are labelled along the bottom. Red represents upregulated genes. Green represents downregulated genes. Black represents unchanged expression.

Table 1: Mouse and human oligonucleotide PCR primer sequences

Gene	Primer Sequence (5' → 3')	
	Forward	Reverse
KIM-1 (Human)	GAAGTGGCTACTGGTTCATGG	ACGACTGTTCGAACGAGCAC
Kim-1 (Mouse)	TCAGCATCTCTAAGCGTGGT	ATGTTGTCTTCAGCTCGGGA
GAPDH (Human)	CCCGTCTAGAAAAACCTGCCA	CGCTTGACAAAGTGGTCGTTG
GAPDH (Mouse)	AGGTCGGTGTGAACGGATTTG	TGTAGACCATGTAGTTGAGGTCA

Table 2: Gene set enrichment and pathway analysis with significant differences between Kim-1$^+$ and Kim-1^{neg} Renca cell lines.

Description	Enrichment Score	P-value
ECM-receptor interaction	11.3631	1.16E-05
Hypertrophic cardiomyopathy (HCM)	11.032	1.62E-05
Dilated cardiomyopathy (DCM)	8.88913	0.00013788
Focal adhesion	6.79961	0.00111421
Neuroactive ligand-receptor interaction	6.64861	0.00129582
Steroid hormone biosynthesis	5.9528	0.00259855
Transcriptional misregulation in cancer	5.09699	0.00611513
PI3K-Akt signaling pathway	4.8097	0.00815028
Arrhythmogenic right ventricular cardiomyopathy (ARVC)	4.51049	0.010993
Taurine and hypotaurine metabolism	4.42065	0.0120265
Rap1 signaling pathway	4.41238	0.0121263
Cytokine-cytokine receptor interaction	4.40875	0.0121704
Systemic lupus erythematosus	4.26625	0.0140343
Intestinal immune network for IgA production	4.10358	0.0165135
Protein digestion and absorption	4.07493	0.0169934
FoxO signaling pathway	3.54657	0.0288234
Cell adhesion molecules (CAMs)	3.29848	0.0369392
Histidine metabolism	3.21793	0.0400379
ABC transporters	3.12373	0.0439929
Taste transduction	2.90685	0.0546475
Arginine and proline metabolism	2.8592	0.0573146
Melanoma	2.83061	0.0589767

* Pathway highlighted in yellow was determined to be the most relevant to invasion and metastasis and will be investigated further

Table 3: Genes with significant fold-change differences between Kim-1$^+$ and Kim-1^{neg} Renca cell lines.

Gene ID	Total Gene Counts	P-value (Kim vs. Ctrl)	Fold change (Kim vs. Ctrl)
Sort1	3.84E+00	0.002407	-78.27
Rab27b	6.19E+01	0.000000	-30.40
Gm44505	1.89E+00	0.003090	-28.77
Plekha5	1.24E+00	0.028411	-16.08
Tmem38b	2.92E+02	0.000654	-9.52
Dcc	1.34E+00	0.038756	-8.93
Mir6236	2.02E+03	0.000902	-7.33
Dmd	1.07E+01	0.000024	-7.28
Nxf7	1.32E+00	0.037429	-6.88
Mir6240	1.69E+01	0.000975	-6.77
Snord34	2.34E+00	0.008322	-6.09
Gm5662	1.28E+00	0.040134	-5.73
Lars2	4.80E+03	0.000390	-5.39
Cyp3a41b	1.42E+00	0.026172	-5.13
Raet1c	4.67E+00	0.000203	5.36
Pcp4	4.74E+00	0.000046	5.77
Gm6639	1.14E+00	0.042225	10.39
Mtss1l	9.89E-01	0.042141	16.35
Rorb	2.70E+00	0.006705	24.49
Asdurf	2.79E+00	0.000478	266.77

* Gene highlighted in yellow was determined to be the most relevant to invasion and metastasis and will be investigated further

Chapter 4

4 Discussion

4.1 Major Findings

4.1.1 KIM-1 inhibits invasion of Renca and 786-O cells *in vitro*

Overall, our *in vitro* studies suggest KIM-1 inhibits the invasive potential of RCC cells. In the migration assay, Kim-1$^+$ Renca cells migrated far less than their Kim-1^{neg} Renca counterparts both in the presence and absence of complete media with 10% FBS (Figure 3A). However, there appears to have been greater numbers of migrated cells in the FBS group compared with the SFM group. From the Renca invasion assay, the addition of FBS did not appear to elicit any differences in migration (Figure 3B). This may be due to the fact that Matrigel contains many proteins and growth factors such as collagen IV, laminin, epidermal growth factor, fibroblast growth factor, and TGF-β, among many others (Hughes, Postovit et al. 2010). The abundance of these growth factors could potentially diminish the chemotactic effect of the FBS medium in the plate wells.

In contrast, there were no observed differences in the number of migrated cells between 786-O shcontrol and 786-O shKIM-1 in the migration assay (Figure 4A). Similar to the Renca migration assay however, the FBS chemoattractant group had increased numbers of migrated cells. Interestingly, in the invasion assay, significantly fewer 786-O shcontrol cells invaded compared with the 786-O shKIM-1 cells in both the SFM group and the FBS group (Figure 4B). These results were unexpected as we predicted that both the migration and invasion assays would reflect what was observed in the Renca cells. We also expected the FBS group to elicit a greater chemotactic response compared with the SFM group. A possible explanation for the difference observed between the SFM group and the 10% group is that the calf serum used exerts inhibitory effects on the invasive potential of human 786-O cells in the presence of matrix proteins. In contrast to our experiment design, others used FBS containing media only when performing 786-O cell invasion assays (Chang, Chen et al. 2011, Zhao, Luo et al. 2015). Overall, our data has led us to conclude that KIM-1 expression on Renca and 786-O cells inhibits invasion *in vitro*. This conclusion is consistent with what had been reported by Cuadros et al. who showed that 786-O cells with

enhanced KIM-1 shedding results in increased invasiveness *in vitro* (Cuadros, Trilla et al. 2013).

4.1.2 KIM-1 expression inhibits the extravasation of RCC cells out of the capillaries

Our CAM experiments demonstrated that KIM-1 expression significantly inhibited the extravasation of RCC cells (Figure 5). In both human 769-P cells and murine Renca cells, the KIM-1-expressing group showed reduced extravasation capabilities. Our results here, however, contradict findings from a recent study demonstrating that KIM-1 overexpression in 769-P cells resulted in increased proliferation but showed mixed results in terms of migration (Cuadros, Trilla et al. 2014). The study found that migration in KIM-1 overexpressing cells was delayed at early time points but proceeded to migrate faster than control cells at later time points. Our results clearly demonstrate that KIM-1 inhibits the invasive potential of 769-P and Renca cells in an *in vivo* model, and suggests an inhibitory role for KIM-1 in cancer cell extravasation.

4.1.3 Longer time points are required for spontaneous metastasis models

Our data from the pilot spontaneous metastasis experiment were inconclusive as there were no significant differences between the Kim-1$^+$ and Kim-1^{neg} groups (Figure 7). In both groups (n=4), only one mouse developed meaningful counts of metastatic nodules. Our lack of results is likely due to insufficient time for metastases to develop post-injection as well as decreased tumour load. We followed the protocol described by Feldman et. al. (2016) who also studied renal metastases to the lungs by Renca cells in mice given regular or high-salt diets (Feldman, Ding et al. 2016), however, we injected 2×10^5 cells instead of 2.5×10^5 cells. In their study, Feldman et al. sacrificed the mice 14 days after Renca cell implantation into the subcapsular space of the kidneys. Injection into the subcapsular space is a commonly accepted method for assessing renal metastasis and has been found to be the most advantageous site for RCC implantation (Naito, von Eschenbach et al. 1986, Matin, Sharma et al. 2010). A recent study injected RCC cells directly into the kidney, but extended the end-point to 23 days before harvesting the lungs (Murphy, James et al. 2017). This study also proposed the use of luciferase-expressing Renca cells so that

bioluminescent imaging (BLI) could be used to visualize and quantify the growth and spread of cancer cells. We have generated luciferase-expressing Renca cells in our laboratory to repeat these experiments so that we can utilize BLI.

4.1.4 KIM-1-mediated inhibition of metastasis occurs independent of adaptive immunity

Using a murine experimental metastasis model, we showed that Kim-1 expression on Renca cells inhibited metastasis of cancer cells to the lungs (Figure 6). Our experimental metastasis data suggest that Kim-1 expression inhibits mechanisms involved in the arrest and extravasation of Renca cells out of the vasculature and into the lungs. When we repeated the experimental metastasis model in immune-deficient (Rag1$^{-/-}$ BALB/c) mice, we found that the differences between KIM-1 expression persisted in the absence of an adaptive immune system in these mice. KIM-1^{+} RCC cells developed significantly fewer metastatic lung nodules compared with KIM-1^{neg} cells in both the murine (Renca) and human (786-O) models, demonstrating that KIM-1 expression results in decreased metastatic potential (Figure 8). Our data indicate that the KIM-1-mediated inhibition of metastasis is inherent to the cancer cells themselves, and not a by-product of the adaptive immune system targeting KIM-1^{+} cells in a more efficient way. Thus, the metastatic phenotype is driven by a loss of KIM-1 expression in RCC cells.

Our lab demonstrated that during renal ischemia-reperfusion injury and phagocytosis, KIM-1 binds to $G\alpha_{12}$ and suppresses its activity (Ismail, Zhang et al. 2015, Ismail, Zhang et al. 2016). $G\alpha_{12}$ has been demonstrated to promote proliferation and metastasis in RCC through various pathways (Lee, Yang et al. 2009, Hashimoto, Mikami et al. 2016). GTP-bound-$G\alpha_{12}$ can bind to EFA6, which can go on to activate the Arf6-EFA6 pathway resulting in EMT (Hashimoto, Mikami et al. 2016). $G\alpha_{12}$ has also been shown to promote the expression of TGF-β1 through a Rho/Rac-dependent pathway, which ultimately leads to the induction of invasion and EMT (Lee, Yang et al. 2009). Rho-GTPases are downstream effectors of $G\alpha_{12}$ and are crucial to the processes of actin remodeling and invasion (Braga, Del Maschio et al. 1999, Lozano, Betson et al. 2003, Miles, Pruitt et al. 2008). Findings made by Ismail et. al. regarding $G\alpha_{12}$ have implications for metastasis in

RCC. For instance, the inhibition of $G\alpha_{12}$ by KIM-1 would result in the inhibition of downstream Rho, which results in the inhibition of invasive properties in tumour cells.

Our current findings regarding KIM-1 in RCC contrast that of several groups who have claimed that KIM-1 promotes tumour growth and exacerbates cancer progression. Microvascular invasion (MVI) is defined by the invasion of cancer cells into the endothelial walls of small blood vessels and is associated with higher risks of metastases and death in patients with ccRCC (Eisenberg, Cheville et al. 2013, Santiago-Agredano, Alvarez-Kindelan et al. 2013). Mijuskovic et. al. (2018) showed that high degrees of MVI were associated with significantly increased expression of tumour tissue KIM-1, and that urinary KIM-1 was associated with worse disease prognoses and higher TNM staging (Mijuskovic, Stanojevic et al. 2018). Their study therefore suggests that KIM-1 is associated with greater risks of invasion and metastases in patients with ccRCC. A recent study has also suggested that KIM-1 silencing in 786-O cells results in tumour growth inhibition (Xu, Sun et al. 2018). Xu et al. found that silencing KIM-1 decreased proliferation *in vitro* and *in vivo*, suggesting KIM-1 is tumourigenic. In this study, KIM-1-knocked-down 786-O cells injected into nude mice developed smaller tumours compared with control 786-O cells – which endogenously expressed KIM-1.

4.1.5   KIM-1 as a tumourigenic molecule

Multiple studies have also identified KIM-1 as a possible early biomarker for the detection of clear cell and papillary RCC, and associated its expression with the disease's tumour grade (Han, Alinani et al. 2005, Zhang, Mashni et al. 2014, Mijuskovic, Stanojevic et al. 2018). One study demonstrated an association between urinary KIM-1 and tumour KIM-1, suggesting that high levels of urinary KIM-1 are indicative of worse prognosis and higher tumour-node-metastasis (TNM) grades (Mijuskovic, Stanojevic et al. 2018). The same study demonstrated that urinary KIM-1 levels were significantly reduced post-nephrectomy, again suggesting a link between urinary KIM-1 and disease progression. Another study found that KIM-1 was expressed on the majority of clear cell, papillary, and metastatic RCC tumours, and may serve as a diagnostic marker for these renal cancers (Lin, Zhang et al. 2007). It has also been previously shown that KIM-1 expression in human 769-P cells promotes tumour growth through the activation of the IL-6/STAT3/HIF-1α

axis, and the silencing of the gene results in reduced proliferation and angiogenesis (Cuadros, Trilla et al. 2014). Studies have demonstrated that KIM-1 promotes tumourigenesis by increasing the secretion of tumour-promoting factors such as TGF-β and IL-6 (Bostrom, Lindgren et al. 2013, Sabbiseti 2014). Elevated TGF-β expression has been associated with the loss of VHL, and has been implicated in the processes of invasion and EMT (Bostrom, Lindgren et al. 2013). Furthermore, it is well established that the majority of ccRCC have a loss-of-function mutation in the VHL gene, which leads to the accumulation of HIF and the subsequent increase in VEGF and other angiogenic factors (De, Otterstatter et al. 2014, Kumar and Gabrilovich 2014, Schodel, Grampp et al. 2016). Taken together, our findings about the role of KIM-1 in RCC pathogenesis are in stark contrast with what had been suggested to be the role of KIM-1 in RCC. Although these studies appear to contradict our findings, they merely focus on a different side of the same coin. The studies focused on the proliferation and progression of the primary tumour as well as the overall disease, but our data assessed the metastatic aspect of the disease and suggests a role for KIM-1 in regulating the metastatic cascade.

4.1.6   Rap1 and Rab27B may be regulated by KIM-1

In this study, we wanted to elucidate the mechanism by which KIM-1 inhibits metastasis in RCC. Utilizing RNA-sequencing, we were able to determine genes and pathways that are differentially expressed between Kim-1^{+} and Kim-1^{neg} Renca cells (Figure 9). Analysis of the data through the Partek Flow software allowed us to narrow down genes and pathways that were significantly different between the cell types. We set stringency values to only include p-values < 0.05. The list of significantly different gene pathways is shown in Table 2. From the gene pathways, we found that the Rap1 signaling pathway is highly involved in the processes of invasion and metastasis (Caron 2003, Shah, Brock et al. 2019). Rap1 is a small GTPase part of the Ras protein family and serves as a regulator of cellular functions such as adhesion, and integrin activation (Zhang, Wang et al. 2017). Rap1 has also been implicated in regulating cadherin-mediated adhesion between endothelial cells to form adherens junctions and strengthen cell attachment (Pannekoek, Kooistra et al. 2009). It has been suggested that Rap1 antagonizes Ras-mediated proliferation and transformation independently via its complex signaling pathway. Rap1 exhibits pleiotropic

effects in different cancers, exerting oncogenic effects in melanoma, breast cancer, and B-cell lymphomas (Gao, Feng et al. 2006, Lin, Tan et al. 2010, McSherry, Brennan et al. 2011), and tumour suppressor effects in bladder, lung, and brain cancers (Lyle, Raaijmakers et al. 2008, Zhang, Wang et al. 2017). The regulation of adherens junctions and actin remodeling by Rap1 have implicated it in the progression of metastasis. Rap1-GAP (GTPase-activating proteins) is known to inactivate Rap1 by converting GTP-bound Rap1 to GDP-bound Rap1 (Kim, Gersey et al. 2012). Evidence suggests that Rap1 promotes invasion and metastasis in RCC, and Rap1-GAP is downregulated in RCC. In contrast, another study demonstrated that Rap1-GAP levels vary between human RCC cell lines, and is moderately expressed in 786-O cell lines relative to 6 other RCC cell lines, suggesting that 786-O cells are relatively less invasive (Wu, Zhang et al. 2011). Taken together, we have speculated a role for Rap1 in the invasion and metastasis of Renca cells which should be further explored to determine whether it is upregulated or downregulated, and whether the metastatic phenotype in Kim-1^{neg} cells is due to upstream effects of Kim-1 on the Rap1 pathway.

When we analyzed the RNA-seq data for specific genes that had significant fold-changes between Kim-1^{+} and Kim-1^{neg} Renca cells, we found that Rab27B displayed a significant decrease in fold-change in Kim-1^{+} cells compared with Kim-1^{neg} cells (Table 3). Like Rap1, Rab27B is a member of the Ras-family of GTPases, and has been shown to be involved in proliferation and invasion in several cancers, with their downregulation conferring reduced invasiveness and improved prognoses (Li, Jin et al. 2017, Yang, Ye et al. 2017, Wu, Niu et al. 2019). In lung adenocarcinoma studies, Rab27B expression was significantly higher in cancer cells compared with noncancerous cell lines, and has been suggested as a negative prognostic marker for lymph node metastasis and TNM staging (Zhang, Fan et al. 2018). Studies have suggested that Rab27B regulates the phosphatidylinositol 3 kinase (PI3K)/AKT pathway in hepatocellular carcinoma (Yang, Ye et al. 2017). The PI3K/AKT pathway has been shown to regulate multiple aspects of cancer including metastasis (Manning and Cantley 2007), and has also been implicated in RCC and is known to be highly activated in the disease (Guo, German et al. 2015). Interestingly, a recent study investigated Rab27A and Rab27B (the 2 subunits of Rab27) and demonstrated that Rab27A − but not Rab27B − was significantly associated with TNM

staging and could serve as a potential prognostic marker for RCC (An, Song et al. 2019). In context with our findings, another possible mechanism could be that Kim-1 downregulates Rab27B, resulting in decreased proliferation and invasion of Renca cells. The role of Rab27B in RCC is unclear, but it may serve as a promising target to focus future research on.

4.2 Limitations

4.2.1 Transwell migration and invasion assays

Transwell chemo-invasion assays were developed over two decades ago and continue to serve as a quick and quantitative model to study invasive cell migration and cell interactions with basement membranes (Albini and Noonan 2010). It remains a relevant model for investigating cancer cell invasiveness *in vitro* as it has been demonstrated that only tumourigenic cells are able to penetrate Matrigel layers (Albini and Noonan 2010, Hughes, Postovit et al. 2010). Serum-free media was used in these pilot experiments to assess the baseline migration of the cells relative to FBS – a standard chemotactic agent in Transwell assays. Fetal bovine serum is one of the most well-known and widely used serums, and contains a multitude of macromolecules, nutrients, attachment and dissemination factors, as well as hormones and growth factors (Shah 1999, Gstraunthaler 2003). It is often used as a supplement in cell culture, and as a chemotactic agent in migration and invasion assays for RCC (Liu, Zhang et al. 2016, Huang, Wei et al. 2017). This is in line with the standard method found in the literature, which typically uses FBS containing medium as the chemoattractant in the plate wells. Additionally, SFM controls are not typically necessary for migration and invasion assays. To elicit more profound and physiologically relevant responses, the addition of chemokines or conditioned media is sometimes used in place of FBS (Justus, Leffler et al. 2014, Jeong, Han et al. 2016, Gabrielyan, Neumann et al. 2017). It has been reported that media conditioned from fibroblasts or cells of choice contribute cytokines, growth factors, metabolites, and ECM proteins to the media, which offer greater growth and chemotactic capacities for cells (Jeong, Han et al. 2016). Alternatively, some studies stimulate cells with chemokines or engineer chemokine overexpression prior to seeding in the Transwell insert to upregulate migratory processes (Xuan, Feng et al. 2017, Zhuang, Cao et al. 2018).

A major limitation of the Transwell assay as a method to study extravasation is that it is only an *in vitro* model and can only investigate the invasiveness of cancer cells at the Matrigel interface. As such, it only simulates 2D interactions between cancer cells and the Matrigel over circular pores and offers a limited scope of what occurs in 3D at tight endothelial junctions *in vivo* during arrest (Kim, Williams et al. 2016). Additionally, the effect of hemodynamics and plasma proteins on migrating cells cannot be investigated using this model as the *in vitro* model lacks the full repertoire of cell types present in the blood. Another limitation is that the time points set for incubation are arbitrary and are not representative of the invasion process *in vivo* which is not as forgiving if cells fail to migrate across the endothelium.

4.2.2   CAM extravasation assay

The CAM extravasation assay overcame the limitations of the Transwell assay by providing a rapid and quantitative assessment of extravasation in an *in vivo* model. The assay was conducted by Marie Sarabusky, who followed the protocol for the CAM extravasation model as described (Kim, Williams et al. 2016). The assay allowed us to specifically investigate the ability of cancer cells to arrest and extravasate out of capillaries into surrounding tissues. It also allowed us to visualize the process of extravasation by using fluorescent dyes to label the cells and the vasculature. Additionally, the low cost of this assay allowed for greater sample sizes with adequate power and allowed for the valid determination of statistical significance.

However, a limitation of the CAM assay is that the use of fluorescently labelled cells – a technique that requires relatively more complex and expensive equipment – is fundamental for visualizing the extravasation of cancer cells from the blood vessels (Kim, Williams et al. 2016). Another limitation to consider is the fact that this model was designed to investigate extravasation of mammalian cells but is applied in an avian embryo. Certain plasma proteins, hormones, and growth factors specific to mammalian cells may not be present in this model. There may not be a complete repertoire of human and mouse accessory proteins and growth factors in the chicken embryo, which could have potentially modulated the phenotypes we observed. Finally, expertise with IV injections is a necessity for the implantation procedure.

4.2.3   Experimental metastasis model

The *in vivo* experimental metastasis model is a relevant model to investigate metastasis and the interaction of molecules with the endothelium of blood vessels (Gomez-Cuadrado, Tracey et al. 2017). The use of this experimental metastasis model allowed us to specifically study the late stages of the metastatic cascade: the arrest and extravasation of cancer cells into the lungs. Renal cell carcinoma preferentially metastasizes to the lungs, so this model was relevant in understanding the effect of KIM-1 expression during extravasation.

A major limitation of the experimental metastasis assay (the IV tail injection model specifically) when it comes to studying metastasis is that it only recapitulates the late stages of the metastatic cascade; arrest and extravasation out of the capillaries into the lungs (Gomez-Cuadrado, Tracey et al. 2017). This assay evaluates how cancer cells grow in ectopic sites but cannot account for how the primary tumour develops and invades into the vasculature.

4.2.4   Spontaneous metastasis model

The spontaneous metastasis model implants the cancer cells orthotopically and overcomes some of the limitations of the experimental model. It mimics the human disease and allows for the development of the primary tumour and its dissemination to secondary sites (Gomez-Cuadrado, Tracey et al. 2017). However, a drawback is that the earliest steps of tumour formation cannot be assessed as the tumours do not spontaneously arise. Transgenic mice allow for the autochthonous development of tumours which recapitulate the entire metastatic cascade and allow for the study of cancer progression using experimental models (Kabeer, Beverly et al. 2016, Gomez-Cuadrado, Tracey et al. 2017). For example, mice engineered with a mutant p53 gene develop normally but are prone to spontaneous tumour formation (Donehower, Harvey et al. 1992). Alternative methods utilize the Cre recombinase/*lox P* system to activate specific oncogenes or inactivate specific tumour suppressors and control the timing for tumour initiation (Jackson, Willis et al. 2001, Gomez-Cuadrado, Tracey et al. 2017). *Lox P* recombination sites flank genes of interest through homologous recombination, which can then be excised when the Cre recombinase

is activated (Gu, Zou et al. 1993). A second limitation is that murine kidneys are quite small, so expertise is required when injecting the cells under the subcapsular space to avoid leakage of cells under the capsule or out of the kidneys. Furthermore, it is impossible to measure the growth of the primary tumour using typical caliper measurements, so BLI will have to be used to quantify tumour growth and dissemination via fluorescent protein signal intensity.

4.2.5   Rag1$^{-/-}$ mice in an experimental metastasis model

Rag1$^{-/-}$ mice lack a functional recombination activation gene (RAG), which prevents them from activating V(D)J recombination early on during T and B cell development (Mombaerts, Iacomini et al. 1992). This recombination is critical to the differentiation of T and B cells, and a deficiency results in mice that have underdeveloped lymphoid organs which lack mature T and B lymphocytes. These mutant mice lack a functional adaptive immune system, thus any observed differences in phenotype can be attributed to KIM-1 expression, and not adaptive immunity.

A major limitation of using Rag1$^{-/-}$ mice is that it knocks out the adaptive immune system (T and B cells) but have an intact natural killer (NK) cell population. NK cells are classically considered innate cells and thought to be activated in response to missing MHC class I molecules on virus-infected or cancer cells, and induce adaptive immune cell activation (Vivier, Tomasello et al. 2008). It has been suggested that NK cells possess anti-tumour properties and inhibit tumour growth and progression early on through various pathways including Fas ligand and granzyme-family proteases. Some studies have shown however, that although NK cells are still present in Rag1-deficient mice, Rag proteins are essential for the functional development and survival of NK cells (Andrews and Smyth 2010, Karo, Schatz et al. 2014). Thus, the Rag1$^{-/-}$ mouse model serves its purpose of studying the effect of the adaptive immune system in KIM-1-mediated inhibition of metastasis. An alternative method would be to perform T and B cell depletion to verify that the observed phenotypes are indeed a result of KIM-1 expression, rather than the adaptive immune system.

4.3 Future Directions and Significance

The implications of our findings within the context of the known literature suggests that KIM-1 expression within tumours may have a paradoxical effect between tumour growth and metastatic ability. On one hand, KIM-1 expression in the tumour promotes proliferation and angiogenesis. On the other hand, KIM-1 expression inhibits the metastasis of the primary tumour cells to distant organs. Although the literature predominantly points towards KIM-1 as tumourigenic, there is evidence to support our data and reconcile the two sides of the coin. A study by Cuadros et. al. (2013) investigated the effect of KIM-1 ectodomain shedding on the invasive capacity of 786-O cells and found that increased shedding ability was directly associated with increased invasiveness and tumour malignancy (Cuadros, Trilla et al. 2013). Their results suggest that surface expression of KIM-1 inhibits invasive properties of RCC cells. An earlier study by Guo et. al. (2012) engineered HT1080 cells that expressed KIM-1, or KIM-1 with a mutated juxtamembrane region which was resistant to shedding by membrane-type-1 matrix metalloprotease (MT1-MMP) (Guo, Takino et al. 2012). They found that the HT1080/KIM-1 cells had their KIM-1 actively cleaved by MT1-MMP, which resulted in significantly increased cell adhesion, invasive growth, and metastasis compared with HT1080/ΔKIM-1 cells. Together with these studies, our work may pave the way for a new hypothesis: although KIM-1 exacerbates tumour growth and progression, the active cleavage of KIM-1 may allow disseminated cancer cells to arrest and invade secondary tissues more efficiently. KIM-1 is overexpressed in >90% of RCC tumours and over a third of patients present with metastases – the primary cause of death in patients with RCC – at the time of diagnosis (Canadian Cancer Society 2015). These facts coupled with our data that indicates KIM-1 inhibits metastasis suggest that KIM-1 is potentially cleaved off RCC cells during their dissemination into the vasculature.

Future work will be aimed at optimizing the spontaneous metastasis model and using Renca-Luciferase cell lines to visualize and quantify tumour growth and metastatic spread via BLI. Optimizing the spontaneous metastasis model will allow us to determine whether the observed phenotypes in the experimental metastasis model are consistently expressed. It will also illuminate whether Kim-1 on RCC cells is shed during its dissemination to the

lungs in a mouse model. We will also explore the effect of anti-Kim-1 antibodies on the development of metastatic lung nodules within both the experimental and spontaneous metastasis model to determine whether blocking Kim-1 in mice injected with Kim-1$^+$ cells will abrogate Kim-1-mediated inhibition of metastasis. Furthermore, Rap1 and Rab27B will be investigated in more detail to determine whether silencing these genes in Kim-1^{neg} Renca cells can block metastasis, and whether Kim-1 inhibits these GTPases like Gα_{12}. Future research could help elucidate the precise mechanism of KIM-1 inhibition and develop specific antagonists that interact with the downstream effectors of KIM-1 in hopes of treating metastatic RCC in patients.

4.4   Conclusion

Our results represent a novel discovery which unveils new perspectives on the relationship between KIM-1 and RCC disease progression. In this study, we hypothesized that KIM-1 expression on RCC cells inhibits their ability to invade and metastasize and our findings are supported by human clinical data (National Cancer Institute 2006). In summary, our work has provided a clearer understanding on the role of KIM-1 in the invasion and metastasis of RCC, and has ultimately provided evidence in support of our hypothesis. We have demonstrated that KIM-1 expression inhibits invasion of Renca and 786-O cells *in vitro*. We have highlighted the inhibitory effect of KIM-1 on the extravasation efficiency of Renca and 769-P cells in an *in vivo* CAM model. We have shown that KIM-1 expression inhibits metastasis in Renca and 786-O cells, and that this inhibitory effect occurs independently from the adaptive immune system. Additionally, we have identified two putative genes (Rap1 and Rab27B) involved in invasion, adhesion, and metastasis that may be regulated by Kim-1. Continued research on the role of KIM-1 in metastatic RCC is likely to substantially enhance our understanding of the pathogenesis of metastatic disease and lead to the development of novel therapeutic targets. The extent of the role that KIM-1 plays in the metastatic cascade of RCC – of which has previously not been studied or discussed within the literature – has thus far been incompletely understood.

Appendices

Appendix A 1: Overall survival between RCC patients with high or low *HAVCR1* expression based on data from TCGA RNA-seq database.

A

B
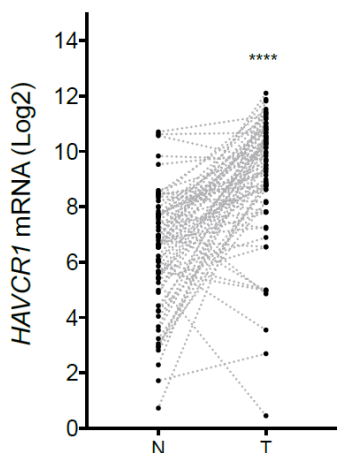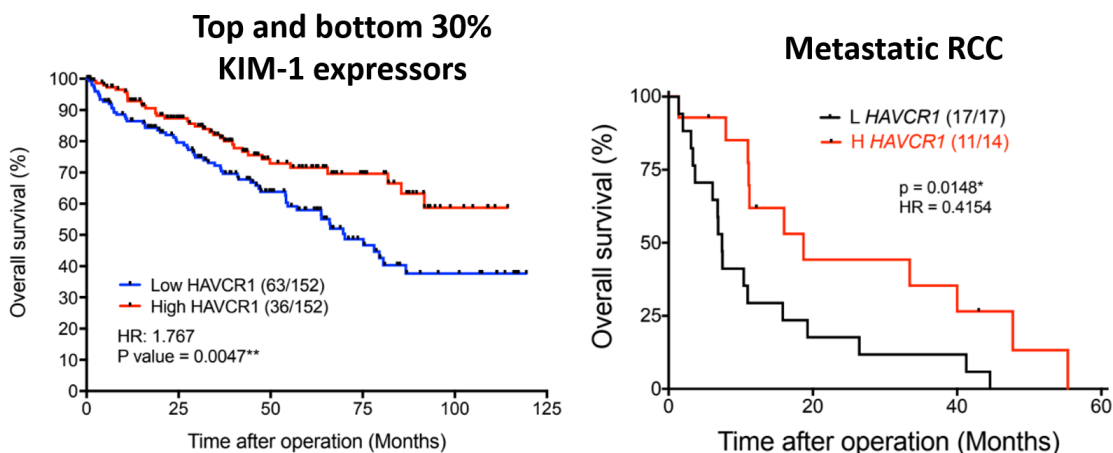
Supplemental Figure 1. Overall survival between RCC patients with high or low *HAVCR1* expression based on data from TCGA RNA-seq database. In renal cell carcinoma (RCC), expression of *HAVCR1* is significantly upregulated in patient specimens but low expression of *HAVCR1* is significantly associated with poor prognosis of RCC patients (P = 0.0034) based on data in The Cancer Genome Atlas. **A)** *HAVCR1* mRNA levels in 72-paired tumour and non-tumour margin tissue specimens of RCC patients obtained from TCGA gene expression profiling datasets are shown. mRNA levels are expressed as individually in tumour vs. non-tumour for each patient. **B)** Kaplan-Meier 10-years (left) or 5-years (right) overall survival curves according to lower versus higher 30% mRNA expression level of *HAVCR1* in TCGA RCC patients.

Appendix A 2: Fekete's Solution

580 mL 100% ethanol

200 mL distilled water

80 mL formalin

40 mL glacial acetic acid

Appendix A 3: Western blots of murine Kim-1 knock-in in the Renca cell line

A   **B**
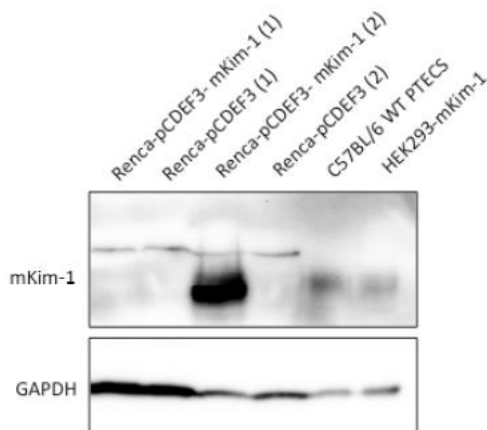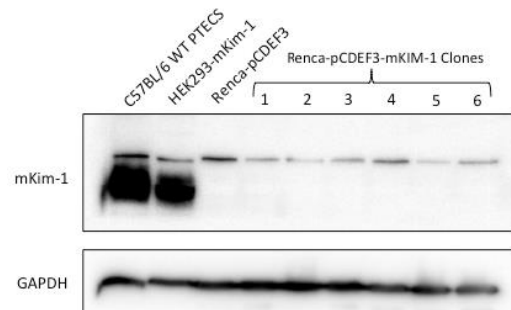
Supplemental Figure 3. Western blots of murine Kim-1 knock-in in the Renca cell line. Renca cells, which do not endogenously express Kim-1, were transfected with either pCDEF3 or pCDEF3-mKim-1 plasmids. **A)** Protein expression in cell lysates from pCDEF3 and pCDEF3-mKim-1 transfected Renca cells were compared to the endogenous protein level of mKim-1 in primary PTECs isolated from WT C57BL/6 mice and to HEK-293 cells transfected with the mKim-1 plasmid. **B)** Renca-pCDEF3 mKim-1 (2) and Renca-pCDEF3 (2) were subjected to G418 selection (400 µg/ml) to select for stable clones expressing mKim-1 or the control plasmid, respectively. Protein lysates from respective Renca clones were compared to the endogenous protein level of Kim-1 in primary PTECs isolated from WT C57BL/6 mice and to HEK-293 cells transfected with the mKim-1 plasmid. WT, wild-type; mKim-1, murine Kim-1; C57BL/6 PTECs, primary proximal tubular epithelial cells isolated from a WT C57BL/6 mouse following kidney injury.

Appendix A 4: Murine Kim-1 expression in the Renca cell line

A   **B**
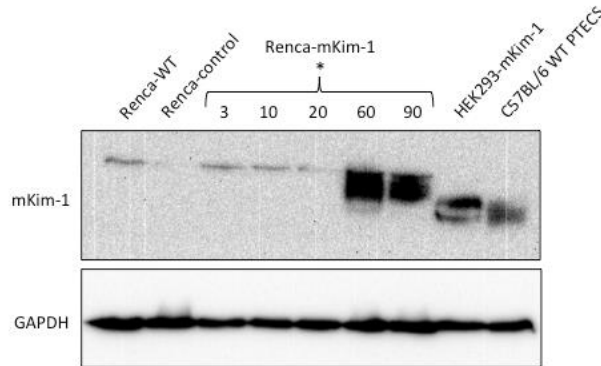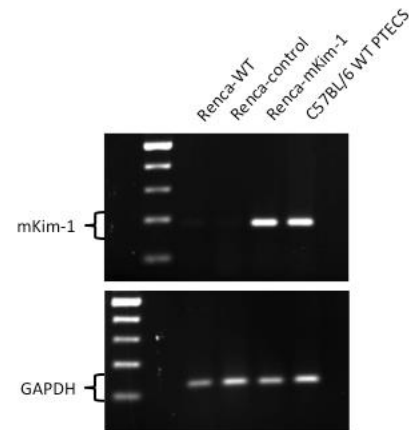
Supplemental Figure 4. Murine Kim-1 expression in the Renca cell line. Renca cells, which do not endogenously express Kim-1**,** were transduced with either lentiviral particles containing the Kim-1 transcript within the vector (Renca-mKim-1) or just the vector alone (Renca-control) and then subjected to selection using puromycin (2 µg/ml) for generation of stable cell lines. **A)** Western blot of protein expression in lysates from Renca-mKIM-1 cells at different MOIs and Renca-control cells (MOI of 60) were compared to the endogenous protein level of mKim-1 in primary PTECs isolated from WT C57BL/6 mice and to HEK-293 cells transfected with the pCDEF3-mKim-1 plasmid. **B)** mRNA expression levels of Kim-1 in Renca-mKim-1 and Renca-control cells transduced with a MOI of 60 were compared to the endogenous mRNA expression level of mKim-1 in primary PTECs isolated from WT C57BL/6 mice using standard PCR as described in the materials and methods. Normalization was performed to GAPDH. WT, wild-type; mKim-1, murine Kim-1; MOI, multiplicity of infection; C57BL/6 PTECs, primary proximal tubular epithelial cells isolated from a WT C57BL/6 mouse following kidney injury.

Appendix A 5: Human KIM-1 knock-down in 769-P cell line

A

B
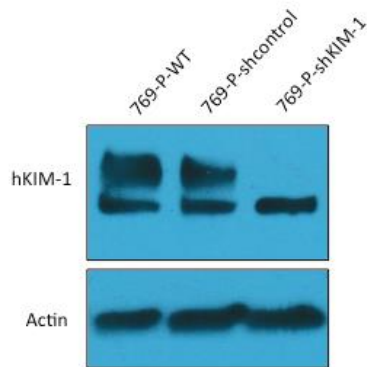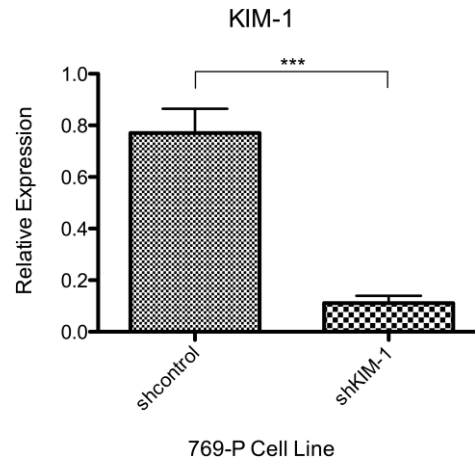
Supplemental Figure 5. Human Kim-1 knockdown in the 769-P cell line. 769-P cells, which endogenously express high levels of KIM-1**,** were transduced with either lentiviral particles containing KIM-1-specific constructs encoding shRNA (shKIM-1) or a scrambled shRNA sequence (shcontrol). **A)** Protein expression in cell lysates from shcontrol and shKIM-1 were compared to the endogenous protein expression level of KIM-1 (769-P WT) by western blotting using antibodies against KIM-1 (extracellular domain) and β-actin. **B)** Relative mRNA expression levels of KIM-1 from total RNA extracted from shcontrol and shKIM-1 cells using real time-PCR (RT-PCR) (n = 9; *** = p < 0.0001). Normalization of KIM-1 was performed to GAPDH and expressed as a fold change. Data is shown as mean ± SEM in the graph. WT, wild-type; hKIM-1, human KIM-1.

References

Albini, A. and D. M. Noonan (2010). "The 'chemoinvasion' assay, 25 years and still going strong: the use of reconstituted basement membranes to study cell invasion and angiogenesis." <u>Curr Opin Cell Biol</u> **22**(5): 677-689.

American Cancer Society, T. (2016). "Cancer facts and figures." from http://www.cancer.org/acs/groups/content/@research/documents/document/acspc-047079.pdf.

An, H. J., D. H. Song, H. M. Koh, G. H. Ko, J. H. Lee, D. C. Kim, J. W. Yang, M. H. Kim, D. H. Seo, S. M. Jang and J. S. Lee (2019). "RAB27A is an independent prognostic factor in clear cell renal cell carcinoma." <u>Biomark Med</u> **13**(4): 239-247.

Andrews, D. M. and M. J. Smyth (2010). "A potential role for RAG-1 in NK cell development revealed by analysis of NK cells during ontogeny." <u>Immunol Cell Biol</u> **88**(2): 107-116.

Arai, S., K. Kitada, T. Yamazaki, R. Takai, X. Zhang, Y. Tsugawa, R. Sugisawa, A. Matsumoto, M. Mori, Y. Yoshihara, K. Doi, N. Maehara, S. Kusunoki, A. Takahata, E. Noiri, Y. Suzuki, N. Yahagi, A. Nishiyama, L. Gunaratnam, T. Takano and T. Miyazaki (2016). "Apoptosis inhibitor of macrophage protein enhances intraluminal debris clearance and ameliorates acute kidney injury in mice." <u>Nat Med</u> **22**(2): 183-193.

Balkwill, F. (2004). "Cancer and the chemokine network." <u>Nat Rev Cancer</u> **4**(7): 540-550.

Bianchi, M., M. Sun, C. Jeldres, S. F. Shariat, Q. D. Trinh, A. Briganti, Z. Tian, J. Schmitges, M. Graefen, P. Perrotte, M. Menon, F. Montorsi and P. I. Karakiewicz (2012). "Distribution of metastatic sites in renal cell carcinoma: a population-based analysis." <u>Ann Oncol</u> **23**(4): 973-980.

Bonventre, J. V. (2014). "Kidney injury molecule-1: a translational journey." <u>Trans Am Clin Climatol Assoc</u> **125**: 293-299; discussion 299.

Bostrom, A. K., D. Lindgren, M. E. Johansson and H. Axelson (2013). "Effects of TGF-beta signaling in clear cell renal cell carcinoma cells." <u>Biochem Biophys Res Commun</u> **435**(1): 126-133.

Braga, V. (2000). "Epithelial cell shape: cadherins and small GTPases." <u>Exp Cell Res</u> **261**(1): 83-90.

Braga, V. M., A. Del Maschio, L. Machesky and E. Dejana (1999). "Regulation of cadherin function by Rho and Rac: modulation by junction maturation and cellular context." <u>Mol Biol Cell</u> **10**(1): 9-22.

Brodaczewska, K. K., C. Szczylik, M. Fiedorowicz, C. Porta and A. M. Czarnecka (2016). "Choosing the right cell line for renal cell cancer research." Mol Cancer **15**(1): 83.

Canadian Cancer Society, T. (2015). "Canadian cancer statistics 2015." from https://www.cancer.ca/~/media/cancer.ca/CW/cancer%20information/cancer%20101/Canadian%20cancer%20statistics/Canadian-Cancer-Statistics-2015-EN.pdf.

Cao, Z., T. Livas and N. Kyprianou (2016). "Anoikis and EMT: Lethal "Liaisons" during Cancer Progression." Crit Rev Oncog **21**(3-4): 155-168.

Caron, E. (2003). "Cellular functions of the Rap1 GTP-binding protein: a pattern emerges." J Cell Sci **116**(Pt 3): 435-440.

Chang, H. R., P. N. Chen, S. F. Yang, Y. S. Sun, S. W. Wu, T. W. Hung, J. D. Lian, S. C. Chu and Y. S. Hsieh (2011). "Silibinin inhibits the invasion and migration of renal carcinoma 786-O cells in vitro, inhibits the growth of xenografts in vivo and enhances chemosensitivity to 5-fluorouracil and paclitaxel." Mol Carcinog **50**(10): 811-823.

Cuadros, T., E. Trilla, E. Sarro, M. R. Vila, J. Vilardell, I. de Torres, M. Salcedo, J. Lopez-Hellin, A. Sanchez, S. Ramon y Cajal, E. Itarte, J. Morote and A. Meseguer (2014). "HAVCR/KIM-1 activates the IL-6/STAT-3 pathway in clear cell renal cell carcinoma and determines tumor progression and patient outcome." Cancer Res **74**(5): 1416-1428.

Cuadros, T., E. Trilla, M. R. Vila, I. de Torres, J. Vilardell, N. B. Messaoud, M. Salcedo, E. Sarro, J. Lopez-Hellin, A. Blanco, C. Mir, S. Ramon y Cajal, E. Itarte, J. Morote and A. Meseguer (2013). "Hepatitis A virus cellular receptor 1/kidney injury molecule-1 is a susceptibility gene for clear cell renal cell carcinoma and hepatitis A virus cellular receptor/kidney injury molecule-1 ectodomain shedding a predictive biomarker of tumour progression." Eur J Cancer **49**(8): 2034-2047.

Custodio, S., A. Joaquim, V. Peixoto, J. E. Macedo, A. L. Faria, E. Macias, S. Rego and A. Araujo (2012). "Metastatic renal cell carcinoma: the importance of immunohistochemistry in differential diagnosis." Case Rep Oncol **5**(1): 30-34.

De, P., M. C. Otterstatter, R. Semenciw, L. F. Ellison, L. D. Marrett and D. Dryer (2014). "7, 1986-2007." Cancer Causes Control **25**(10): 1271-1281.

de Vivar Chevez, A. R., J. Finke and R. Bukowski (2014). "The role of inflammation in kidney cancer." Adv Exp Med Biol **816**: 197-234.

Donehower, L. A., M. Harvey, B. L. Slagle, M. J. McArthur, C. A. Montgomery, Jr., J. S. Butel and A. Bradley (1992). "Mice deficient for p53 are developmentally normal but susceptible to spontaneous tumours." Nature **356**(6366): 215-221.

Dong, H., S. E. Strome, D. R. Salomao, H. Tamura, F. Hirano, D. B. Flies, P. C. Roche, J. Lu, G. Zhu, K. Tamada, V. A. Lennon, E. Celis and L. Chen (2002). "Tumor-

associated B7-H1 promotes T-cell apoptosis: a potential mechanism of immune evasion." Nat Med **8**(8): 793-800.

Dorsam, R. T. and J. S. Gutkind (2007). "G-protein-coupled receptors and cancer." Nat Rev Cancer **7**(2): 79-94.

Edlund, M., S. Y. Sung and L. W. Chung (2004). "Modulation of prostate cancer growth in bone microenvironments." J Cell Biochem **91**(4): 686-705.

Eisenberg, M. S., J. C. Cheville, R. H. Thompson, D. Kaushik, C. M. Lohse, S. A. Boorjian, B. A. Costello and B. C. Leibovich (2013). "Association of microvascular and capillary-lymphatic invasion with outcome in patients with renal cell carcinoma." J Urol **190**(1): 37-43.

Fadok, V. A., J. S. Savill, C. Haslett, D. L. Bratton, D. E. Doherty, P. A. Campbell and P. M. Henson (1992). "Different populations of macrophages use either the vitronectin receptor or the phosphatidylserine receptor to recognize and remove apoptotic cells." J Immunol **149**(12): 4029-4035.

Feldman, R. D., Q. Ding, Y. Hussain, L. E. Limbird, J. G. Pickering and R. Gros (2016). "Aldosterone mediates metastatic spread of renal cancer via the G protein-coupled estrogen receptor (GPER)." FASEB J **30**(6): 2086-2096.

Ferlay, J., I. Soerjomataram, R. Dikshit, S. Eser, C. Mathers, M. Rebelo, D. M. Parkin, D. Forman and F. Bray (2015). "Cancer incidence and mortality worldwide: sources, methods and major patterns in GLOBOCAN 2012." Int J Cancer **136**(5): E359-386.

Fidler, I. J. (2003). "The pathogenesis of cancer metastasis: the 'seed and soil' hypothesis revisited." Nat Rev Cancer **3**(6): 453-458.

Fife, B. T. and J. A. Bluestone (2008). "Control of peripheral T-cell tolerance and autoimmunity via the CTLA-4 and PD-1 pathways." Immunol Rev **224**: 166-182.

Finke, J. H., P. A. Rayman, J. S. Ko, J. M. Bradley, S. J. Gendler and P. A. Cohen (2013). "Modification of the tumor microenvironment as a novel target of renal cell carcinoma therapeutics." Cancer J **19**(4): 353-364.

Francia, G., W. Cruz-Munoz, S. Man, P. Xu and R. S. Kerbel (2011). "Mouse models of advanced spontaneous metastasis for experimental therapeutics." Nat Rev Cancer **11**(2): 135-141.

Gabrielyan, A., E. Neumann, M. Gelinsky and A. Rosen-Wolff (2017). "Metabolically conditioned media derived from bone marrow stromal cells or human skin fibroblasts act as effective chemoattractants for mesenchymal stem cells." Stem Cell Res Ther **8**(1): 212.

Gao, L., Y. Feng, R. Bowers, M. Becker-Hapak, J. Gardner, L. Council, G. Linette, H. Zhao and L. A. Cornelius (2006). "Ras-associated protein-1 regulates extracellular signal-

regulated kinase activation and migration in melanoma cells: two processes important to melanoma tumorigenesis and metastasis." Cancer Res **66**(16): 7880-7888.

Gassmann, P., J. Haier, K. Schluter, B. Domikowsky, C. Wendel, U. Wiesner, R. Kubitza, R. Engers, S. W. Schneider, B. Homey and A. Muller (2009). "CXCR4 regulates the early extravasation of metastatic tumor cells in vivo." Neoplasia **11**(7): 651-661.

Gomez-Cuadrado, L., N. Tracey, R. Ma, B. Qian and V. G. Brunton (2017). "Mouse models of metastasis: progress and prospects." Dis Model Mech **10**(9): 1061-1074.

Gordan, J. D., P. Lal, V. R. Dondeti, R. Letrero, K. N. Parekh, C. E. Oquendo, R. A. Greenberg, K. T. Flaherty, W. K. Rathmell, B. Keith, M. C. Simon and K. L. Nathanson (2008). "HIF-alpha effects on c-Myc distinguish two subtypes of sporadic VHL-deficient clear cell renal carcinoma." Cancer Cell **14**(6): 435-446.

Gstraunthaler, G. (2003). "Alternatives to the use of fetal bovine serum: serum-free cell culture." ALTEX **20**(4): 275-281.

Gu, H., Y. R. Zou and K. Rajewsky (1993). "Independent control of immunoglobulin switch recombination at individual switch regions evidenced through Cre-loxP-mediated gene targeting." Cell **73**(6): 1155-1164.

Gunaratnam, L., M. Morley, A. Franovic, N. de Paulsen, K. Mekhail, D. A. Parolin, E. Nakamura, I. A. Lorimer and S. Lee (2003). "Hypoxia inducible factor activates the transforming growth factor-alpha/epidermal growth factor receptor growth stimulatory pathway in VHL(-/-) renal cell carcinoma cells." J Biol Chem **278**(45): 44966-44974.

Guo, H., P. German, S. Bai, S. Barnes, W. Guo, X. Qi, H. Lou, J. Liang, E. Jonasch, G. B. Mills and Z. Ding (2015). "The PI3K/AKT Pathway and Renal Cell Carcinoma." J Genet Genomics **42**(7): 343-353.

Guo, L., T. Takino, Y. Endo, T. Domoto and H. Sato (2012). "Shedding of kidney injury molecule-1 by membrane-type 1 matrix metalloproteinase." J Biochem **152**(5): 425-432.

Han, W. K., A. Alinani, C. L. Wu, D. Michaelson, M. Loda, F. J. McGovern, R. Thadhani and J. V. Bonventre (2005). "Human kidney injury molecule-1 is a tissue and urinary tumor marker of renal cell carcinoma." J Am Soc Nephrol **16**(4): 1126-1134.

Hanahan, D. and R. A. Weinberg (2011). "Hallmarks of cancer: the next generation." Cell **144**(5): 646-674.

Harlander, S., D. Schonenberger, N. C. Toussaint, M. Prummer, A. Catalano, L. Brandt, H. Moch, P. J. Wild and I. J. Frew (2017). "Combined mutation in Vhl, Trp53 and Rb1 causes clear cell renal cell carcinoma in mice." Nat Med **23**(7): 869-877.

Hashimoto, S., S. Mikami, H. Sugino, A. Yoshikawa, A. Hashimoto, Y. Onodera, S. Furukawa, H. Handa, T. Oikawa, Y. Okada, M. Oya and H. Sabe (2016).

"Lysophosphatidic acid activates Arf6 to promote the mesenchymal malignancy of renal cancer." Nat Commun **7**: 10656.

Hess, K. R., G. R. Varadhachary, S. H. Taylor, W. Wei, M. N. Raber, R. Lenzi and J. L. Abbruzzese (2006). "Metastatic patterns in adenocarcinoma." Cancer **106**(7): 1624-1633.

Huang, W., X. L. Wei, W. Ni, M. Cao, L. Meng and H. Yang (2017). "The expression of RNA-binding protein RBM38 decreased in renal cell carcinoma and represses renal cancer cell proliferation, migration, and invasion." Tumour Biol **39**(5): 1010428317701635.

Hughes, C. S., L. M. Postovit and G. A. Lajoie (2010). "Matrigel: a complex protein mixture required for optimal growth of cell culture." Proteomics **10**(9): 1886-1890.

Humphreys, B. D., F. Xu, V. Sabbisetti, I. Grgic, S. Movahedi Naini, N. Wang, G. Chen, S. Xiao, D. Patel, J. M. Henderson, T. Ichimura, S. Mou, S. Soeung, A. P. McMahon, V. K. Kuchroo and J. V. Bonventre (2013). "Chronic epithelial kidney injury molecule-1 expression causes murine kidney fibrosis." J Clin Invest **123**(9): 4023-4035.

Ichimura, T., E. J. Asseldonk, B. D. Humphreys, L. Gunaratnam, J. S. Duffield and J. V. Bonventre (2008). "Kidney injury molecule-1 is a phosphatidylserine receptor that confers a phagocytic phenotype on epithelial cells." J Clin Invest **118**(5): 1657-1668.

Ichimura, T., J. V. Bonventre, V. Bailly, H. Wei, C. A. Hession, R. L. Cate and M. Sanicola (1998). "Kidney injury molecule-1 (KIM-1), a putative epithelial cell adhesion molecule containing a novel immunoglobulin domain, is up-regulated in renal cells after injury." J Biol Chem **273**(7): 4135-4142.

Ismail, O. Z., X. Zhang, J. V. Bonventre and L. Gunaratnam (2016). "G protein alpha12 (Galpha12) is a negative regulator of kidney injury molecule-1-mediated efferocytosis." Am J Physiol Renal Physiol **310**(7): F607-F620.

Ismail, O. Z., X. Zhang, J. Wei, A. Haig, B. M. Denker, R. S. Suri, A. Sener and L. Gunaratnam (2015). "Kidney injury molecule-1 protects against Galpha12 activation and tissue damage in renal ischemia-reperfusion injury." Am J Pathol **185**(5): 1207-1215.

Jackson, E. L., N. Willis, K. Mercer, R. T. Bronson, D. Crowley, R. Montoya, T. Jacks and D. A. Tuveson (2001). "Analysis of lung tumor initiation and progression using conditional expression of oncogenic K-ras." Genes Dev **15**(24): 3243-3248.

Jeong, D., C. Han, I. Kang, H. T. Park, J. Kim, H. Ryu, Y. S. Gho and J. Park (2016). "Effect of Concentrated Fibroblast-Conditioned Media on In Vitro Maintenance of Rat Primary Hepatocyte." PLoS One **11**(2): e0148846.

Justus, C. R., N. Leffler, M. Ruiz-Echevarria and L. V. Yang (2014). "In vitro cell migration and invasion assays." J Vis Exp(88).

Kabeer, F., L. J. Beverly, G. Darrasse-Jeze and K. Podsypanina (2016). "Methods to Study Metastasis in Genetically Modified Mice." Cold Spring Harb Protoc **2016**(2): pdb top069948.

Karo, J. M., D. G. Schatz and J. C. Sun (2014). "The RAG recombinase dictates functional heterogeneity and cellular fitness in natural killer cells." Cell **159**(1): 94-107.

Khanna, C. and K. Hunter (2005). "Modeling metastasis in vivo." Carcinogenesis **26**(3): 513-523.

Kim, W. J., Z. Gersey and Y. Daaka (2012). "Rap1GAP regulates renal cell carcinoma invasion." Cancer Lett **320**(1): 65-71.

Kim, Y., K. C. Williams, C. T. Gavin, E. Jardine, A. F. Chambers and H. S. Leong (2016). "Quantification of cancer cell extravasation in vivo." Nat Protoc **11**(5): 937-948.

Kobayashi, N., P. Karisola, V. Pena-Cruz, D. M. Dorfman, M. Jinushi, S. E. Umetsu, M. J. Butte, H. Nagumo, I. Chernova, B. Zhu, A. H. Sharpe, S. Ito, G. Dranoff, G. G. Kaplan, J. M. Casasnovas, D. T. Umetsu, R. H. Dekruyff and G. J. Freeman (2007). "TIM-1 and TIM-4 glycoproteins bind phosphatidylserine and mediate uptake of apoptotic cells." Immunity **27**(6): 927-940.

Koh, M. Y. and G. Powis (2012). "Passing the baton: the HIF switch." Trends Biochem Sci **37**(9): 364-372.

Kozlowski, J. M., I. J. Fidler, D. Campbell, Z. L. Xu, M. E. Kaighn and I. R. Hart (1984). "Metastatic behavior of human tumor cell lines grown in the nude mouse." Cancer Res **44**(8): 3522-3529.

Kumar, V. and D. I. Gabrilovich (2014). "Hypoxia-inducible factors in regulation of immune responses in tumour microenvironment." Immunology **143**(4): 512-519.

Kusaba, T., M. Lalli, R. Kramann, A. Kobayashi and B. D. Humphreys (2014). "Differentiated kidney epithelial cells repair injured proximal tubule." Proc Natl Acad Sci U S A **111**(4): 1527-1532.

Lambert, A. W., D. R. Pattabiraman and R. A. Weinberg (2017). "Emerging Biological Principles of Metastasis." Cell **168**(4): 670-691.

Lee, S. J., J. W. Yang, I. J. Cho, W. D. Kim, M. K. Cho, C. H. Lee and S. G. Kim (2009). "The gep oncogenes, Galpha(12) and Galpha(13), upregulate the transforming growth factor-beta1 gene." Oncogene **28**(9): 1230-1240.

Li, J., Q. Jin, F. Huang, Z. Tang and J. Huang (2017). "Effects of Rab27A and Rab27B on Invasion, Proliferation, Apoptosis, and Chemoresistance in Human Pancreatic Cancer Cells." Pancreas **46**(9): 1173-1179.

Lin, F., P. L. Zhang, X. J. Yang, J. Shi, T. Blasick, W. K. Han, H. L. Wang, S. S. Shen, B. T. Teh and J. V. Bonventre (2007). "Human kidney injury molecule-1 (hKIM-1): a useful immunohistochemical marker for diagnosing renal cell carcinoma and ovarian clear cell carcinoma." Am J Surg Pathol **31**(3): 371-381.

Lin, K. B., P. Tan, S. A. Freeman, M. Lam, K. M. McNagny and M. R. Gold (2010). "The Rap GTPases regulate the migration, invasiveness and in vivo dissemination of B-cell lymphomas." Oncogene **29**(4): 608-615.

Liu, T. Y., H. Zhang, S. M. Du, J. Li and X. H. Wen (2016). "Expression of microRNA-210 in tissue and serum of renal carcinoma patients and its effect on renal carcinoma cell proliferation, apoptosis, and invasion." Genet Mol Res **15**(1): 15017746.

Liu, W., H. Li, Y. Wang, X. Zhao, Y. Guo, J. Jin and R. Chi (2017). "MiR-30b-5p functions as a tumor suppressor in cell proliferation, metastasis and epithelial-to-mesenchymal transition by targeting G-protein subunit alpha-13 in renal cell carcinoma." Gene **626**: 275-281.

Lozano, E., M. Betson and V. M. Braga (2003). "Tumor progression: Small GTPases and loss of cell-cell adhesion." Bioessays **25**(5): 452-463.

Lyle, K. S., J. H. Raaijmakers, W. Bruinsma, J. L. Bos and J. de Rooij (2008). "cAMP-induced Epac-Rap activation inhibits epithelial cell migration by modulating focal adhesion and leading edge dynamics." Cell Signal **20**(6): 1104-1116.

Manning, B. D. and L. C. Cantley (2007). "AKT/PKB signaling: navigating downstream." Cell **129**(7): 1261-1274.

Massari, F., M. Santoni, C. Ciccarese, D. Santini, S. Alfieri, G. Martignoni, M. Brunelli, F. Piva, R. Berardi, R. Montironi, C. Porta, S. Cascinu and G. Tortora (2015). "PD-1 blockade therapy in renal cell carcinoma: current studies and future promises." Cancer Treat Rev **41**(2): 114-121.

Matin, S. F., P. Sharma, I. S. Gill, C. Tannenbaum, M. G. Hobart, A. C. Novick and J. H. Finke (2010). "Immunological response to renal cryoablation in an in vivo orthotopic renal cell carcinoma murine model." J Urol **183**(1): 333-338.

McSherry, E. A., K. Brennan, L. Hudson, A. D. Hill and A. M. Hopkins (2011). "Breast cancer cell migration is regulated through junctional adhesion molecule-A-mediated activation of Rap1 GTPase." Breast Cancer Res **13**(2): R31.

Mijuskovic, M., I. Stanojevic, N. Milovic, S. Cerovic, D. Petrovic, D. Maksic, B. Kovacevic, T. Andjelic, P. Aleksic, B. Terzic, M. Djukic and D. Vojvodic (2018). "Tissue and urinary KIM-1 relate to tumor characteristics in patients with clear renal cell carcinoma." Int Urol Nephrol **50**(1): 63-70.

Miles, F. L., F. L. Pruitt, K. L. van Golen and C. R. Cooper (2008). "Stepping out of the flow: capillary extravasation in cancer metastasis." Clin Exp Metastasis **25**(4): 305-324.

Miyake, M., S. Goodison, A. Lawton, G. Zhang, E. Gomes-Giacoia and C. J. Rosser (2013). "Erythropoietin is a JAK2 and ERK1/2 effector that can promote renal tumor cell proliferation under hypoxic conditions." J Hematol Oncol **6**: 65.

Molitoris, B. A. (2014). "Therapeutic translation in acute kidney injury: the epithelial/endothelial axis." J Clin Invest **124**(6): 2355-2363.

Mombaerts, P., J. Iacomini, R. S. Johnson, K. Herrup, S. Tonegawa and V. E. Papaioannou (1992). "RAG-1-deficient mice have no mature B and T lymphocytes." Cell **68**(5): 869-877.

Morton, C. L. and P. J. Houghton (2007). "Establishment of human tumor xenografts in immunodeficient mice." Nat Protoc **2**(2): 247-250.

Murphy, G. P. and W. J. Hrushesky (1973). "A murine renal cell carcinoma." J Natl Cancer Inst **50**(4): 1013-1025.

Murphy, K. A., B. R. James, A. Wilber and T. S. Griffith (2017). "A Syngeneic Mouse Model of Metastatic Renal Cell Carcinoma for Quantitative and Longitudinal Assessment of Preclinical Therapies." J Vis Exp(122).

Naito, S., A. C. von Eschenbach, R. Giavazzi and I. J. Fidler (1986). "Growth and metastasis of tumor cells isolated from a human renal cell carcinoma implanted into different organs of nude mice." Cancer Res **46**(8): 4109-4115.

National Cancer Institute, T. (2006). The Cancer Genome Atlas Program. National Cancer Institute, National Cancer Institute.

Pannekoek, W. J., M. R. Kooistra, F. J. Zwartkruis and J. L. Bos (2009). "Cell-cell junction formation: the role of Rap1 and Rap1 guanine nucleotide exchange factors." Biochim Biophys Acta **1788**(4): 790-796.

Patanaphan, V., O. M. Salazar and R. Risco (1988). "Breast cancer: metastatic patterns and their prognosis." South Med J **81**(9): 1109-1112.

Philips, G. K. and M. B. Atkins (2014). "New agents and new targets for renal cell carcinoma." Am Soc Clin Oncol Educ Book: e222-227.

Raman, R. and D. Vaena (2015). "Immunotherapy in Metastatic Renal Cell Carcinoma: A Comprehensive Review." Biomed Res Int **2015**: 367354.

Raval, R. R., K. W. Lau, M. G. Tran, H. M. Sowter, S. J. Mandriota, J. L. Li, C. W. Pugh, P. H. Maxwell, A. L. Harris and P. J. Ratcliffe (2005). "Contrasting properties of hypoxia-inducible factor 1 (HIF-1) and HIF-2 in von Hippel-Lindau-associated renal cell carcinoma." Mol Cell Biol **25**(13): 5675-5686.

Rennebeck, G., M. Martelli and N. Kyprianou (2005). "Anoikis and survival connections in the tumor microenvironment: is there a role in prostate cancer metastasis?" Cancer Res **65**(24): 11230-11235.

Reymond, N., B. B. d'Agua and A. J. Ridley (2013). "Crossing the endothelial barrier during metastasis." Nat Rev Cancer **13**(12): 858-870.

Sabbiseti, V. S. (2014). KIM-1 is a novel therapeutic target in renal cell carcinoma. American Association for Cancer Research.

Sabbisetti, V. S., S. S. Waikar, D. J. Antoine, A. Smiles, C. Wang, A. Ravisankar, K. Ito, S. Sharma, S. Ramadesikan, M. Lee, R. Briskin, P. L. De Jager, T. T. Ngo, M. Radlinski, J. W. Dear, K. B. Park, R. Betensky, A. S. Krolewski and J. V. Bonventre (2014). "Blood kidney injury molecule-1 is a biomarker of acute and chronic kidney injury and predicts progression to ESRD in type I diabetes." J Am Soc Nephrol **25**(10): 2177-2186.

Sakamoto, S., R. O. McCann, R. Dhir and N. Kyprianou (2010). "Talin1 promotes tumor invasion and metastasis via focal adhesion signaling and anoikis resistance." Cancer Res **70**(5): 1885-1895.

Santiago-Agredano, B., J. Alvarez-Kindelan, P. Font-Ugalde, A. Blanca-Pedregosa, A. Lopez-Beltran and M. J. Requena-Tapia (2013). "Prognostic value of microvascular invasion in predicting survival in renal cell carcinoma." Actas Urol Esp **37**(8): 504-512.

Scelo, G., D. C. Muller, E. Riboli, M. Johansson, A. J. Cross, P. Vineis, K. K. Tsilidis, P. Brennan, H. Boeing, P. H. M. Peeters, R. C. H. Vermeulen, K. Overvad, H. B. Bueno-de-Mesquita, G. Severi, V. Perduca, M. Kvaskoff, A. Trichopoulou, C. La Vecchia, A. Karakatsani, D. Palli, S. Sieri, S. Panico, E. Weiderpass, T. M. Sandanger, T. H. Nost, A. Agudo, J. R. Quiros, M. Rodriguez-Barranco, M. D. Chirlaque, T. J. Key, P. Khanna, J. V. Bonventre, V. S. Sabbisetti and R. S. Bhatt (2018). "KIM-1 as a Blood-Based Marker for Early Detection of Kidney Cancer: A Prospective Nested Case-Control Study." Clin Cancer Res **24**(22): 5594-5601.

Schioppa, T., B. Uranchimeg, A. Saccani, S. K. Biswas, A. Doni, A. Rapisarda, S. Bernasconi, S. Saccani, M. Nebuloni, L. Vago, A. Mantovani, G. Melillo and A. Sica (2003). "Regulation of the chemokine receptor CXCR4 by hypoxia." J Exp Med **198**(9): 1391-1402.

Schodel, J., S. Grampp, E. R. Maher, H. Moch, P. J. Ratcliffe, P. Russo and D. R. Mole (2016). "Hypoxia, Hypoxia-inducible Transcription Factors, and Renal Cancer." Eur Urol **69**(4): 646-657.

Shah, G. (1999). "Why do we still use serum in the production of biopharmaceuticals?" Dev Biol Stand **99**: 17-22.

Shah, S., E. J. Brock, K. Ji and R. R. Mattingly (2019). "Ras and Rap1: A tale of two GTPases." Semin Cancer Biol **54**: 29-39.

Shen, C., R. Beroukhim, S. E. Schumacher, J. Zhou, M. Chang, S. Signoretti and W. G. Kaelin, Jr. (2011). "Genetic and functional studies implicate HIF1alpha as a 14q kidney cancer suppressor gene." Cancer Discov **1**(3): 222-235.

Shimazui, T., J. Oosterwijk-Wakka, H. Akaza, P. P. Bringuier, E. Ruijter, F. M. Debruyne, J. A. Schalken and E. Oosterwijk (2000). "Alterations in expression of cadherin-6 and E-cadherin during kidney development and in renal cell carcinoma." Eur Urol **38**(3): 331-338.

Shinojima, T., M. Oya, A. Takayanagi, R. Mizuno, N. Shimizu and M. Murai (2007). "Renal cancer cells lacking hypoxia inducible factor (HIF)-1alpha expression maintain vascular endothelial growth factor expression through HIF-2alpha." Carcinogenesis **28**(3): 529-536.

Staller, P., J. Sulitkova, J. Lisztwan, H. Moch, E. J. Oakeley and W. Krek (2003). "Chemokine receptor CXCR4 downregulated by von Hippel-Lindau tumour suppressor pVHL." Nature **425**(6955): 307-311.

Stoletov, K., H. Kato, E. Zardouzian, J. Kelber, J. Yang, S. Shattil and R. Klemke (2010). "Visualizing extravasation dynamics of metastatic tumor cells." J Cell Sci **123**(Pt 13): 2332-2341.

Su, D., L. Stamatakis, E. A. Singer and R. Srinivasan (2014). "Renal cell carcinoma: molecular biology and targeted therapy." Curr Opin Oncol **26**(3): 321-327.

Teicher, B. A. and S. P. Fricker (2010). "CXCL12 (SDF-1)/CXCR4 pathway in cancer." Clin Cancer Res **16**(11): 2927-2931.

Thompson, R. H., H. Dong and E. D. Kwon (2007). "Implications of B7-H1 expression in clear cell carcinoma of the kidney for prognostication and therapy." Clin Cancer Res **13**(2 Pt 2): 709s-715s.

Vivier, E., E. Tomasello, M. Baratin, T. Walzer and S. Ugolini (2008). "Functions of natural killer cells." Nat Immunol **9**(5): 503-510.

White, R. V. and D. A. Olsson (1980). "Renal adenocarcinoma in the rat: a new tumor model." Invest Urol **17**(5): 405-412.

Wirtz, D., K. Konstantopoulos and P. C. Searson (2011). "The physics of cancer: the role of physical interactions and mechanical forces in metastasis." Nat Rev Cancer **11**(7): 512-522.

Wu, G., M. Niu, J. Qin, Y. Wang and J. Tian (2019). "Inactivation of Rab27B-dependent signaling pathway by calycosin inhibits migration and invasion of ER-negative breast cancer cells." Gene **709**: 48-55.

Wu, J., Y. Zhang, N. Frilot, J. I. Kim, W. J. Kim and Y. Daaka (2011). "Prostaglandin E2 regulates renal cell carcinoma invasion through the EP4 receptor-Rap GTPase signal transduction pathway." J Biol Chem **286**(39): 33954-33962.

Xu, J., L. Sun, W. Sun, J. Tian and H. Guo (2018). "Targeted Silencing of Kim-1 Inhibits the Growth of Clear Cell Renal Cell Carcinoma Cell Line 786-0 In Vitro and In Vivo." Oncol Res **26**(7): 997-1003.

Xuan, W., X. Feng, C. Qian, L. Peng, Y. Shi, L. Xu, F. Wang and W. Tan (2017). "Osteoclast differentiation gene expression profiling reveals chemokine CCL4 mediates RANKL-induced osteoclast migration and invasion via PI3K pathway." Cell Biochem Funct **35**(3): 171-177.

Yagi, H., W. Tan, P. Dillenburg-Pilla, S. Armando, P. Amornphimoltham, M. Simaan, R. Weigert, A. A. Molinolo, M. Bouvier and J. S. Gutkind (2011). "A synthetic biology approach reveals a CXCR4-G13-Rho signaling axis driving transendothelial migration of metastatic breast cancer cells." Sci Signal **4**(191): ra60.

Yang, L., C. R. Brooks, S. Xiao, V. Sabbisetti, M. Y. Yeung, L. L. Hsiao, T. Ichimura, V. Kuchroo and J. V. Bonventre (2015). "KIM-1-mediated phagocytosis reduces acute injury to the kidney." J Clin Invest **125**(4): 1620-1636.

Yang, X., X. Ye, L. Sun, F. Gao, Y. Li, X. Ji, X. Wang, Y. Feng and X. Wang (2017). "Downregulation of serum RAB27B confers improved prognosis and is associated with hepatocellular carcinoma progression through PI3K-AKT-P21 signaling." Oncotarget **8**(37): 61118-61132.

Zagzag, D., B. Krishnamachary, H. Yee, H. Okuyama, L. Chiriboga, M. A. Ali, J. Melamed and G. L. Semenza (2005). "Stromal cell-derived factor-1alpha and CXCR4 expression in hemangioblastoma and clear cell-renal cell carcinoma: von Hippel-Lindau loss-of-function induces expression of a ligand and its receptor." Cancer Res **65**(14): 6178-6188.

Zargarian, S., I. Shlomovitz, Z. Erlich, A. Hourizadeh, Y. Ofir-Birin, B. A. Croker, N. Regev-Rudzki, L. Edry-Botzer and M. Gerlic (2017). "Phosphatidylserine externalization, "necroptotic bodies" release, and phagocytosis during necroptosis." PLoS Biol **15**(6): e2002711.

Zhang, L., W. Fan, L. Xu, Q. Mao, Y. Chen, Y. Mao, L. Xu and J. Wang (2018). "Rab27b Is a Potential Indicator for Lymph Node Metastasis and Unfavorable Prognosis in Lung Adenocarcinoma." Dis Markers **2018**: 7293962.

Zhang, P. L., J. W. Mashni, V. S. Sabbisetti, C. M. Schworer, G. D. Wilson, S. C. Wolforth, K. M. Kernen, B. D. Seifman, M. B. Amin, T. J. Geddes, F. Lin, J. V. Bonventre and J. M. Hafron (2014). "Urine kidney injury molecule-1: a potential non-invasive biomarker for patients with renal cell carcinoma." Int Urol Nephrol **46**(2): 379-388.

Zhang, Y. L., R. C. Wang, K. Cheng, B. Z. Ring and L. Su (2017). "Roles of Rap1 signaling in tumor cell migration and invasion." <u>Cancer Biol Med</u> **14**(1): 90-99.

Zhao, C. X., C. L. Luo and X. H. Wu (2015). "Hypoxia promotes 786-O cells invasiveness and resistance to sorafenib via HIF-2alpha/COX-2." <u>Med Oncol</u> **32**(1): 419.

Zhu, J., C. Liang, Y. Hua, C. Miao, J. Zhang, A. Xu, K. Zhao, S. Liu, Y. Tian, H. Dong, C. Zhang, P. Li, S. Su, C. Qin and Z. Wang (2017). "The metastasis suppressor CD82/KAI1 regulates cell migration and invasion via inhibiting TGF-beta 1/Smad signaling in renal cell carcinoma." <u>Oncotarget</u> **8**(31): 51559-51568.

Zhu, Z., O. Sanchez-Sweatman, X. Huang, R. Wiltrout, R. Khokha, Q. Zhao and E. Gorelik (2001). "Anoikis and metastatic potential of cloudman S91 melanoma cells." <u>Cancer Res</u> **61**(4): 1707-1716.

Zhuang, H., G. Cao, C. Kou and T. Liu (2018). "CCL2/CCR2 axis induces hepatocellular carcinoma invasion and epithelial-mesenchymal transition in vitro through activation of the Hedgehog pathway." <u>Oncol Rep</u> **39**(1): 21-30.

Zimmerman, M., X. Hu and K. Liu (2010). "Experimental metastasis and CTL adoptive transfer immunotherapy mouse model." <u>J Vis Exp</u>(45).

Curriculum Vitae

Name:	Jasper Christiano Lee

Post-secondary Education and Degrees:

B.M.Sc. in Medical Sciences
Honours Specialization in Interdisciplinary Medical Sciences
Western University
London, Ontario, Canada
2012-2017

M.Sc. in Microbiology and Immunology
Western University
London, Ontario, Canada
2017-2019

Related Work Experience

Graduate Teaching Assistant
Genetics 2581
Western University
London, Ontario, Canada
2017-2018

Graduate Teaching Assistant
Microbiology and Immunology 3620
Western University
London, Ontario, Canada
2018-2019